

1 **β-catenin perturbations control differentiation programs in mouse embryonic
2 stem cells**

3 Elisa Pedone^{1,2,+}, Mario Failli^{3,4}, Gennaro Gambardella^{3,4}, Rossella De Cegli³, Diego
4 di Bernardo^{3,4} and Lucia Marucci^{1,2,5,+}.

5 ¹Department of Engineering Mathematics, University of Bristol, Bristol BS8 1UB, UK. ²School
6 of Cellular and Molecular Medicine, University of Bristol, Bristol BS8 1TD, UK. ³Telethon
7 Institute of Genetic and Medicine Via Campi Flegrei 34, 80078 Pozzuoli, Italy. ⁴Department of
8 Chemical, Materials and Industrial Production Engineering, University of Naples Federico II,
9 80125 Naples, Italy. ⁵BrisSynBio, Bristol BS8 1TQ, UK.

10 ⁺ corresponding authors; elisa.pedone@bristol.ac.uk; lucia.marucci@bristol.ac.uk

11

12 **Abstract**

13 The Wnt/β-catenin pathway is involved in development, cancer and embryonic stem
14 cell (ESC) maintenance; its dual role in stem cell self-renewal and differentiation is still
15 controversial. Here, we applied an elegant *in vitro* system enabling conditional β-
16 catenin control in β-catenin null mouse ESCs. We report that moderate induction of
17 exogenous β-catenin enhances epiblast stem cell (EpiSC) derivation *in vitro*. Using a
18 different genetic model and β-catenin chemical modulation, we derived a new protocol
19 for ESCs to EpiSCs differentiation, based on NDif227 and the GSK3α/β inhibitor
20 Chiron, that is more efficient than standard ActivinA/Fgf2-based protocols. Finally, we
21 report that moderate β-catenin levels favour early stem cell commitment towards
22 mesoderm if the protein is overexpressed only in the ‘ground state’ of pluripotency
23 conditions, or endoderm if the overexpression is maintained during the differentiation,
24 unravelling the controversial role of this signalling pathway at the exit from
25 pluripotency.

26

27 **Introduction**

28 Pluripotent Cells (PCs) are characterized by indefinite proliferative and differentiation
29 potential and their identity is determined by the balance between signals promoting
30 self-renewal and differentiation. The first step for stem cell differentiation is the exit
31 from the pluripotent state, tightly controlled by underlying gene regulatory network
32 dynamics which can drive specific lineage commitment. During murine development
33 *in vivo*, embryonic stem cells (ESCs), that represent the naïve pluripotent state of the
34 early epiblast¹⁻³, convert into the late epiblast and finally in terminally differentiated

35 somatic cells. ESCs can be derived from the pre-implantation epiblast and used to
36 study cell pluripotency and differentiation, providing an excellent *in vitro* system for
37 understanding signalling pathway interplay in cell fate decision making.

38 In serum-based cultures, mouse ESCs (hereafter called ESCs) are heterogeneous for
39 the expression of pluripotency genes^{1,2,4-10}, while, when cultured in serum-free media
40 supplemented with inhibitors of MEK1/2 (PD) and GSK3α/β (Chiron) and in presence
41 or not of the Leukaemia Inhibitory Factor-LIF (2i or 2i+LIF)³, a uniform self-renewal
42 condition known as 'ground state' of pluripotency is established; it is characterized by
43 homogenous gene expression¹¹⁻¹⁴, genome demethylation¹⁵⁻¹⁷ and stable naïve
44 pluripotency^{18,19}. Mouse epiblast stem cells (hereafter called EpiSCs) also represent
45 a relevant *in vitro* model because of their similarities with embryonic stem cells of
46 human origin²⁰. EpiSCs, derived from the post-implantation epiblast, are also capable
47 of differentiating in all the germ-layers^{20,21}; however, they differ from ESCs in
48 morphology, clonogenicity, gene expression, epigenome status and, most importantly,
49 ability to contribute to chimaeras^{14,20-22}. EpiSCs require ActivinA and the fibroblast
50 growth factor 2 (FGF2)^{20,21} for *in vitro* expansion; of note, FGF signalling pathway
51 activation, while promoting EpiSC self-renewal, induces ESC differentiation^{23,24}.
52 FGF2 treatment, in combination or not with ActivinA and LIF/STAT3 pathway
53 inhibitors, has been used for ESCs differentiation into EpiSCs both in serum-based
54 and serum-free culture conditions²⁵⁻²⁸, although with low efficiency. Self-renewing
55 EpiSCs have been recently established by simultaneous activation and inhibition of
56 the Wnt/β-catenin pathway²⁹; however, the effect of these perturbations on ESCs-
57 EpiSCs direct transition has not been fully explored.

58

59 The Wnt/β-catenin is a highly conserved signalling pathway involved in ESCs self-
60 renewal³⁰ and cell-cycle progression³¹. β-catenin levels are tightly controlled by the
61 active transcription of negative regulators working at different levels of the signalling
62 cascade³²: Axin2³³⁻³⁵ is part of the disruption complex whereas DKK1³⁶ binds the Wnt
63 receptor complex attenuating cellular response upon activation of the pathway. These
64 negative feedback loops contribute to the emergence of nonlinear dynamics in the
65 Wnt/β-catenin pathway, proved to be important in different biological and
66 developmental aspects (as reviewed in³⁷), ESCs pluripotency¹⁰ and somatic cell
67 reprogramming^{10,38-41}. The role of the canonical Wnt pathway in early *in vivo*
68 developmental stages and the requirement of its activation for ESC self-renewal have

69 been a matter of intense research, often generating contradictory results^{3,42-47}.
70 Pluripotency incompetence has been reported in two independent studies using β -
71 catenin^{-/-} ECSS^{42,44}; this phenotype was, however, contradicted in later studies with
72 newly generated β -catenin^{-/-} cell lines, which normally self-renew in both serum and
73 2i+LIF (hereafter called 2i/L), but present some differentiation defects when LIF-
74 deprived⁴⁵⁻⁴⁷. Such knock-out models provide an excellent *in vitro* system to study β -
75 catenin function on ESC decision making.

76

77 Here, we take advantage of the β -catenin^{-/-} ESC line generated by Aulicino and
78 colleagues⁴⁵, where the entire β -catenin coding sequence was removed to avoid
79 possible compensatory mechanisms from aberrant truncated isoforms, to study the
80 effect of β -catenin perturbations on the exit from pluripotency and differentiation.
81 Different β -catenin doses have been indirectly achieved in the past by mutating the
82 adenomatous polyposis coli gene (APC)⁴⁸; teratomas from the mutants with the
83 highest β -catenin transcriptional activity showed major differentiation defects in the
84 neuroectoderm, dorsal mesoderm and endoderm lineages. Of note, results in⁴⁸
85 suggest that active β -catenin nuclear translocation (different across mutants) might
86 also be involved in the observed differentiation impairment. Cellular models enabling
87 direct modulation of β -catenin are necessary to systematically associate protein
88 perturbations to pluripotency and differentiation phenotypes.

89 We tuned β -catenin levels in β -catenin^{-/-} ESCs applying an improved inducible
90 system⁴⁹ and measured both the global gene expression following 2i/L withdrawal,
91 and the efficiency of ESC-EpiSC transition *in vitro*. Comparing the response to
92 differentiation stimuli of ESCs expanded in serum/LIF or 2i/L, we demonstrated that
93 moderate β -catenin overexpression in β -catenin^{-/-} ESCs enhances the differentiation
94 efficiency into EpiSCs. Moreover, short-term expansion in 2i/L predisposes ESCs to
95 such transition, challenging the hypothesis of a synergistic effect of the ERK, Wnt/ β -
96 catenin and STAT pathways on EpiSCs derivation *in vitro* that would require further
97 investigation. These results were recapitulated by exposing wild-type ESCs to low
98 doses of the GSK3 α/β inhibitor Chiron, further confirming our findings and providing
99 an improved protocol for fast and efficient *in vitro* derivation of EpiSCs. Finally, the
100 transcriptome of ESCs expressing different β -catenin levels confirmed what we and
101 others reported about β -catenin dispensable requirement for pluripotency

102 establishment^{45-47,49}, while suggesting that specific β -catenin perturbations cause a
103 bias towards the endoderm lineage.

104 Overall, our study highlights that synergistic effects of β -catenin doses and culture
105 conditions control *in vitro* ESC fate decision making.

106

107 **Results**

108

109 **Wnt/ β -catenin pathway perturbations control *in vitro* generation of EpiSC**

110 To study the role of the Wnt/ β -catenin pathway in EpiSC derivation *in vitro*, we used
111 the C1-EF1a-rtTA_TRE3G-DDmCherry β -catenin^{S33Y} (hereafter called C1) ESC line
112 we previously generated⁴⁹. Briefly, β -catenin^{-/-} ESCs⁴⁵ were modified to stably
113 express a doxycycline-inducible fusion protein comprising the conditional destabilising
114 domain (DD), the mCherry fluorescent protein and the constitutive active β -
115 catenin^{S33Y}(Figure 1A)⁵⁰. The inducer molecule doxycycline (Dox) enables
116 transcriptional initiation, while trimethoprim (TMP) allows protein stabilisation by
117 inactivating the DD (Figure 1A)⁴⁹. The use of a constitutively active and conditional β -
118 catenin^{S33Y} form, uncoupled from upstream endogenous regulations and in a knock-
119 out background, would help in dissecting β -catenin functions in the ESC-EpiSC
120 transition, avoiding compensatory mechanisms and possible off-target effects of
121 stable over-expression and chemical compounds.

122 We confirmed, in C1 cells, the correct induction (Figure 1A, inset and⁴⁹), intracellular
123 distribution and functionality of the exogenous protein upon input administration⁴⁹. We
124 previously confirmed the dispensable role of β -catenin in pluripotent culture conditions
125 and showed, using Alkaline Phosphatase Staining, that moderate β -catenin
126 overexpression (i.e., TMP10 μ M_Doxy10ng/mL) can protect cells from exiting
127 pluripotency in the absence of both serum and LIF⁴⁹. Following these results, we
128 measured the efficiency of EpiSCs derivation when different doses of exogenous β -
129 catenin are overexpressed in pluripotent conditions and/or during differentiation,
130 adapting an existing differentiation protocol^{29,51} (see Methods for details). To
131 appreciate cellular response changes depending on the culture condition, C1 ESCs
132 were expanded either in serum/LIF (hereafter called FBS/L) or in 2i/L. ESCs in the
133 'ground state' media (i.e. 2i/L)³ have been extensively characterised for their
134 transcriptional and epigenetic homogeneity^{12,14} and resemblance of the pre-
135 implantation epiblast^{11,15-18}. However, prolonged culture in 2i/L results in epigenetic

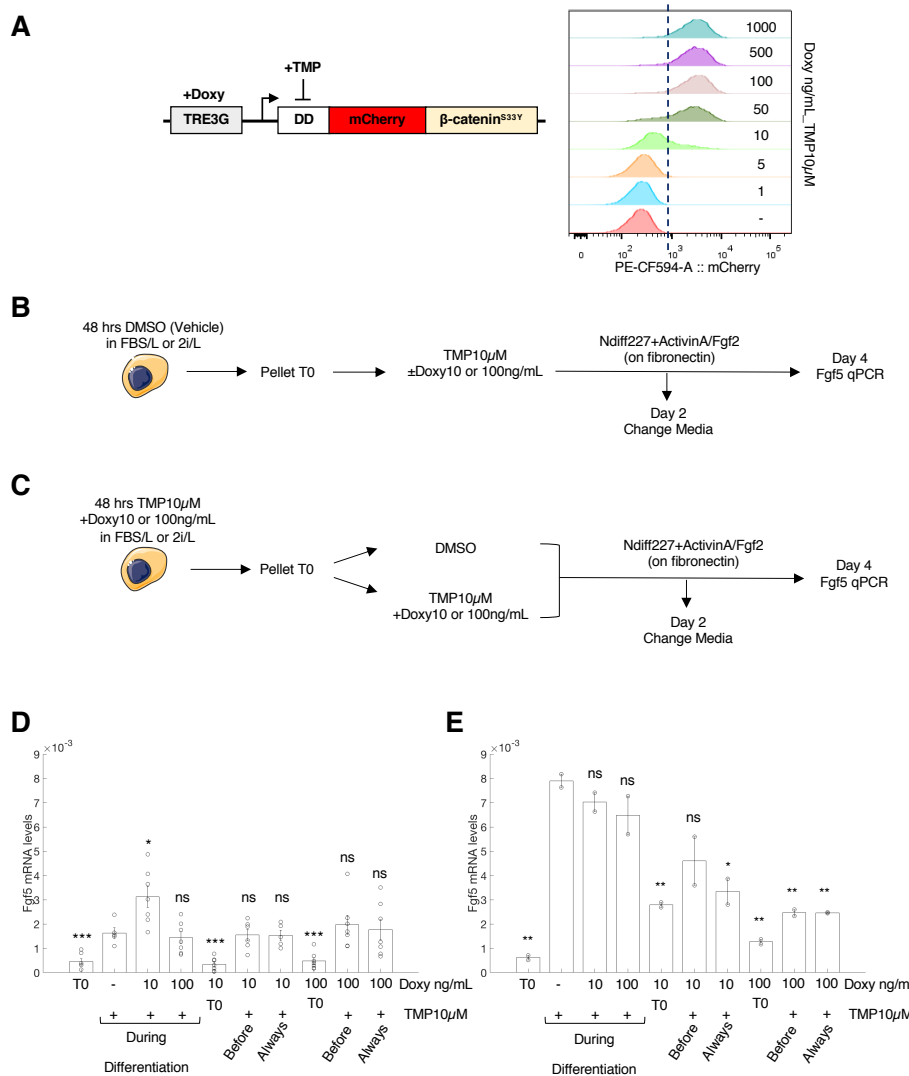
136 changes impairing normal differentiation *in vitro* and development *in vivo*⁵². Therefore,
137 we opted for a short-term culture in 2i/L (3 passages), sufficient to obtain cell
138 homogeneity while avoiding possible aberrations.

139 ESCs from FBS/L or 2i/L (Figure 1B, C) were cultured for 48 hrs either in DMSO
140 (Figure 1B) or in presence of maximum TMP (10µM) combined with low (10ng/mL) or
141 saturating (100ng/mL) Doxy (Figure 1C). The concentrations of Doxy were
142 extrapolated from flow cytometry measurements of the mCherry signal to provide two
143 doses (moderate and high) of the exogenous protein (Figure 1A, inset). We next
144 seeded 1.5×10^4 cells/cm² on fibronectin-coated plates in NDiff227²⁶ supplemented
145 with ActivinA, FGF2²⁹ and different combinations of DMSO, TMP and Doxy (Figure
146 1B, C and Methods). Cells kept under these conditions for 4 days, with media
147 refreshed after the first 2 culture days, were subsequently analysed for the expression
148 of the Epiblast marker Fgf5 by qPCR (Figure 1B, C).

149 TMP/Doxy pre-treatment before differentiation (Figure 1C) did not alter the basal Fgf5
150 expression of FBS/L ESCs (T0 samples in Figure 1D), whereas that of
151 TMP10µM_Doxy10ng/mL treated ESCs from 2i/L culture was higher compared to the
152 TMP10µM_Doxy100ng/mL and the TMP10µM treated samples (T0 samples in Figure
153 1E).

154 Upon 4 days of differentiation, in all Doxy/TMP treated conditions, Fgf5 levels were
155 higher when C1 ESCs were pre-cultured in 2i/L, suggesting that the latter predisposes
156 cells to more efficiently differentiate into EpiSCs (Figure 1E). In both scenarios (i.e.,
157 from FBS/L or 2i/L), β -catenin overexpression in pluripotent conditions only (i.e.,
158 “Before” in Figure 1D, E), or both before and during differentiation (i.e., “Always” in
159 Figure 1D, E), did not increase Fgf5 levels as compared to the control (i.e. TMP10µM-
160 treated C1 ESCs, Figure 1D, E). Interestingly, FBS/L pre-cultured C1 ESCs induced
161 with a low amount of Doxy (TMP10µM_Doxy10ng/mL “During Differentiation” sample,
162 Figure 1D) converted into EpiSCs more efficiently as compared to all other treatments
163 from FBS/L (Figure 1D).

164 Altogether, these results indicate that both the cell culture media and the doses of
165 exogenous β -catenin strongly influence how cells respond to the ActivinA/FGF2
166 differentiation stimulus, with the 2i/L pre-culture enabling more homogeneous
167 differentiation towards Epiblast, and moderate β -catenin overexpression in FBS/L-
168 derived ESCs during the differentiation protocol only improving EpiSCs establishment
169 *in vitro*.



170 **Figure 1. Dual-input control of β-catenin doses in EpiSC derivation *in vitro*.**

171 **A** Dual-input regulation system consisting of the doxycycline responsive element and the
172 conditionally destabilised mCherryβ-catenin^{S33Y} module. Doxycycline (Dox) and trimethoprim
173 (TMP) allow mCherryβ-catenin^{S33Y} transcription initiation and protein stabilisation,
174 respectively. **(A, inset)** Flow cytometry profile of C1 ESCs treated for 24 hrs with TMP10μM
175 and the indicated concentrations of Doxy. **B, C** Experimental scheme ESC to EpiSC
176 differentiation. FBS/L and 2i/L C1 ESCs were pre-treated either with DMSO (**B**) or TMP10μM
177 and Doxy10-100ng/mL (**C**). Following 48 hrs of treatment, cells were seeded on fibronectin in
178 NDiff227 and exposed to ActivinA/FGF2 and different combination of DMSO, Doxy and TMP
179 for 4 days before being collected for RNA extraction. After 2 days, the media was changed,
180 and the drugs were refreshed. **D, E** Fgf5 mRNA levels measured in FBS/L (**D**) and 2i/L (**E**)
181 C1 ESCs, after 4 days of differentiation in NDiff227+ActivinA/FGF2 and different combination
182 of DMSO, Doxy and TMP. Data are means±SEM (n=7, D (T0, Doxy10-100ng/mL “During
183 Differentiation”, Doxy10ng/mL T0, Doxy100ng/mL T0, Doxy100ng/mL “Before” ad
184 Doxy100ng/mL “Always”); n=6, D (Dox10ng/mL “Before”); n=5, D (TMP10μM “During

185 Differentiation"); n=2, E). p-values from two-tailed unpaired t test computed by comparing each
186 sample with C1 TMP10 μ M "During Differentiation" are shown, *p<0.05, **p<0.01, ***p<0.001,
187 ****p<0.0001. Dots represent individual data with similar values overlapping.

188

189 **Chemical modulation of the canonical Wnt pathway enhances Epiblast 190 derivation from ESCs**

191 The above results (Figure 1) and the need to define a protocol for efficient derivation
192 of EpiSCs *in vitro* motivated us to explore the differentiation potential of wild-type ESCs
193 when deprived of pluripotency factors and exposed to different chemical perturbations
194 of the Wnt/β-catenin pathway (Figure 2A). We took advantage of the *miR-290-*
195 *mCherry/miR-302-eGFP*⁵³ ESC line (hereafter called dual reporter ESCs), which
196 allows fluorescent tracking of the exit from pluripotency. Specifically, naïve dual
197 reporter ESCs express the mCherry reporter only, and progressively start expressing
198 also the GFP reporter when allowed to differentiate into EpiSCs⁵³.

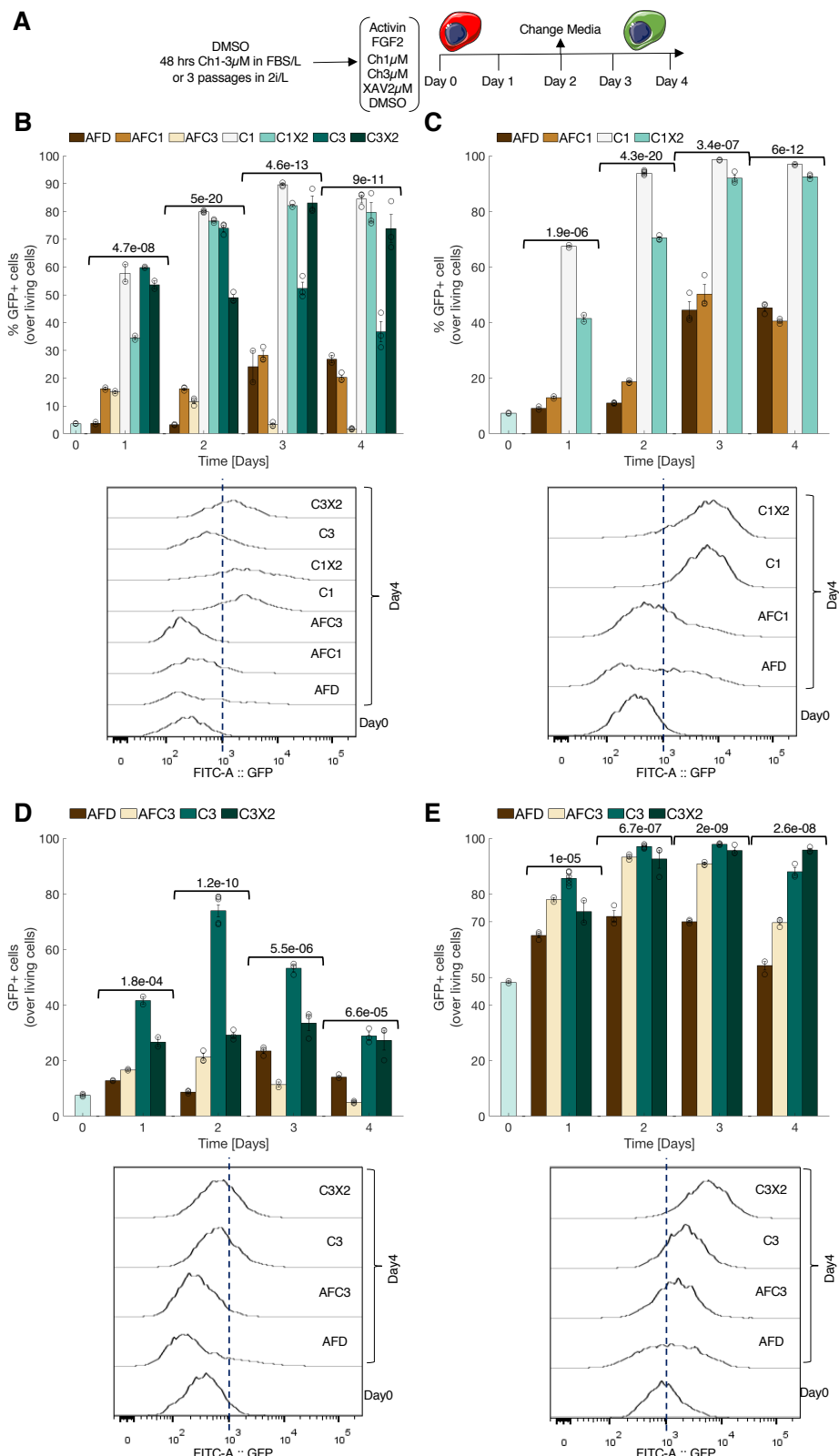
199 We measured the transition from ESCs to EpiSCs using flow cytometry in at least 2
200 independent 4-day time-courses (Figure 2A). Before differentiation, dual reporter
201 ESCs were cultured in FBS/L and treated for 48 hrs with DMSO (Figure 2B) or with
202 Chiron (1-3 μ M, Figure 2C, D respectively) to pre-activate the canonical Wnt pathway,
203 or were maintained in 2i/L for 3 passages (i.e., 1 week; Figure 2E). At Day 0, 1.5 \times 10⁴
204 cells/cm² were seeded on fibronectin-coated plates and exposed to different
205 combination of drugs added to the NDiff227²⁶: ActivinA+FGF2+DMSO (AFD);
206 ActivinA+FGF2+Ch1 μ M (AFC1); ActivinA+FGF2+Ch3 μ M (AFC3); Ch1 μ M (C1);
207 Ch1 μ M+XAV2 μ M (C1X2); Ch3 μ M (C3); Ch3 μ M+XAV2 μ M²⁹ (C3X2) (Figure 2A). The
208 GFP signal was analyzed using flow cytometry every day for 4 days and the media
209 changed after the first 2 culture days (Figure 2A).

210 Dual reporter ESCs pre-cultured in FBS/L in absence of β-catenin activation showed,
211 already at Day 1, a GFP+ cell percentage increase in all but AFD treatment; AFD-
212 treated cells efficiently transited towards the Epi state later in the experiment, but they
213 were unable to reach other treatment GFP+ percentage levels (Figure 2B).

214 FBS/L Ch1 μ M pre-cultured dual reporter ESCs showed an overall increased
215 percentage of GFP+ cells compared to DMSO-treated ESCs (compare Figure 2B, C).
216 However, the fold-increase at Day 4 with respect to Day 0 of the best performing
217 conditions (i.e., C1 and C1X2; Figure 2C) was lower in Ch1 μ M pre-treated cells (13-
218 and 12-fold increase, respectively; Figure 2C) in comparison with the DMSO (23- and

219 22-fold increase, respectively; Figure 2B). This suggests, as in the experiments
220 performed in a β -catenin null background (Figure 1), that the ESC to EpiSC conversion
221 is favoured by β -catenin activation during the differentiation only, while its prolonged
222 stimulation might reduce the differentiation efficiency. This was confirmed in Ch3 μ M
223 pre-treated cells, where the best performing conditions (i.e., C3 and C3X2; Figure 2D)
224 also showed an overall lower percentage of GFP+ cells as compared to DMSO-treated
225 ESCs. Moreover, the simultaneous activation/inhibition of the pathway (i.e., C3X2
226 condition) had opposite effects given cells pre-culture conditions: the percentage of
227 GFP+ cells increased over-time in DMSO pre-treated cells (20-fold increase at Day 4
228 with respect to Day 0; Figure 2B), while GFP expression was quite low at the end of
229 the time-course in Ch3 μ M pre-treated ESCs (3.6-fold increase at Day 4 with respect
230 to Day 0; Figure 2D). Interestingly, Chiron pre-treatment had no positive effect on the
231 differentiation efficiency using the standard differentiation protocol (AFD), as the GFP+
232 percentage increase in AFD-treated cells at Day 4, as compared to Day 0, was almost
233 the same in Ch1 μ M pre-cultured cells (7.4-fold increase; Figure 2C) and lower in
234 Ch3 μ M (1.9-fold increase; Figure 2D) and 2i/L (1.1-fold increase; Figure 2E) pre-
235 cultured cells as compared to the DMSO condition (7.4-fold increase; Figure 2B). In
236 ESCs pre-cultured in 2i/L, there was not much difference across the differentiation
237 protocols, as can be seen by the overall higher p-values computed through a one-way
238 ANOVA test (compare Figure 2B-E). Finally, the combined treatment with ActivinA,
239 FGF2 and Chiron (AFC1 and AFC3; Figure 2B-E) did not change EpiSCs derivation
240 efficiency, as compared to the standard ActivinA/FGF2 treatment (Figure 2B-E).
241 The ESC-EpiSC transition was proven to be a highly heterogeneous process involving
242 massive cell death⁵⁴. Although we did not observe significant changes in cell viability
243 across experiments, we noticed strong variability in the efficiency of *in vitro* EpiSCs
244 derivation: in Supplementary Figure 2, we show the average of at least 2 experiments
245 where the overall percentage of GFP+ cells was almost halved across conditions, as
246 compared to data in Figure 2. Still, results in Supplementary Figure 2 confirm that the
247 addition of Chiron during differentiation, in combination or not with XAV2 μ M (C1 and
248 C1X2 or C3 and C3X2; Supplementary Figure 2A-D), enables a much more efficient
249 conversion towards EpiSCs as compared to the other protocols. Also, we confirmed
250 that, if pre-cultured in FBS/L, no pre-activation of the Wnt/ β -catenin pathway and
251 differentiation in media enriched with Ch1 μ M or Ch1 μ M \pm XAV2 μ M enables efficient

252 EpiSCs derivation (C1 and C1X2; Supplementary Figure 2A), in agreement with β -
 253 catenin genetic perturbation results in Figure 1.



254 **Figure 2. Chemical perturbation of the Wnt/ β -catenin in EpiSC derivation *in vitro*.**
 255 **A** Experimental scheme of Epiblast differentiation. Dual reporter ESCs cultured in FBS/L and
 256 pre-treated for 48 hrs with DMSO and Chiron (1-3 μ M), or in 2i/L for 3 passages, were seeded

257 on fibronectin in NDiff227 supplemented with different combination of drugs
258 (ActivinA+FGF2+DMSO (AFD); ActivinA+FGF2+Ch1 μ M (AFC1); ActivinA+FGF2+Ch3 μ M
259 (AFC3); Ch1 μ M (C1); Ch1 μ M+XAV2 μ M (C1X2); Ch3 μ M (C3); Ch3 μ M+XAV2 μ M (C3X2)). The
260 GFP signal from the EpiSC marker was measured by flow cytometry every 24 hrs for 4
261 consecutive days. After the first 2 days, the media was changed, and the drugs were
262 refreshed. **B-E** Percentage of GFP+ cells calculated over the total amount of living cells in
263 DMSO (**B**), Ch1 μ M (**C**), Ch3 μ M (**D**) and 2i/L (**E**) pre-cultured dual reporter ESCs. Histograms
264 from Day 0 and Day 4 of each condition are shown as insets. Data are means \pm SEM (n=2, B
265 (Day1, Day3 AFD, Day4 AFD), C (Day 1), D (Day1, Day3 AFC3), E (Day0, Day1 AFC3-C3X2);
266 n=3, B (Day0, Day2, Day3 AFC1-AFC3-C1-C1X2-C3-C3X2, Day4 AFC1-AFC3-C1-C1X2-
267 C3-C3X2), C (Day0, Day2 AFD-AFC1-C1X2, Day3, Day4), D (Day0, Day2 AFD-AFC3-C3X2,
268 Day3 AFD-C3-C3X2, Day4), E (Day1 AFD, Day2 AFD-AFC3-C3X2, Day3, Day4); n=6, C
269 (Day2 C1), D (Day2 C3), E (Day1 C3, Day2 C3). p-values from one-way ANOVA are shown
270 across samples for each day. Dots represent individual data with similar values overlapping.
271 Colour-blind safe combinations were selected using colorbrewer2
272 (<https://colorbrewer2.org/#type=sequential&scheme=BuGn&n=3>).
273

274 To confirm these results at single cell level, we monitored single-cell ESC-EpiSC
275 transition in 71 hrs time-lapse microscopy experiments (Supplementary Movies 1-3;
276 see Methods for details). FBS/L pre-cultured dual reporter ESCs were imaged every
277 60 minutes while constantly stimulated with AFD (Supplementary Movie 1) or Chiron
278 1-3 μ M (Supplementary Movies 2 and 3, respectively). In the AFD condition, a few
279 GFP+ cells started to appear after 57 hrs (Supplementary Movie 1), whereas in the
280 C1 and C3 culture conditions the transition started already after 10-14 hrs, with a peak
281 around 40-43 hrs (Supplementary Movies 2 and 3). The GFP signal from cells
282 differentiated in the presence of Chiron3 μ M was weaker as compared to the
283 Chiron1 μ M treatment (compare Supplementary Movies 2 and 3).

284 These results confirm that strength and time of β -catenin stabilization are important to
285 tip the balance between cell fates. In agreement with our previous observations in
286 FBS/L pre-cultured knock-out cells (see TMP10 μ M_Doxy10ng/ml “During
287 Differentiation” sample in Figure 1D), data collected using the dual reporter cell line
288 confirm that high levels of β -catenin can be detrimental to efficiently derive EpiSCs *in*
289 *vitro*. Indeed, a moderate activation or the simultaneous treatment with both an
290 activator (i.e., Chiron) and an inhibitor (i.e., XAV) of the Wnt/ β -catenin pathway

291 improve ESC direct differentiation into EpiSC, effectively replacing ActivinA and FGF2
292 requirement (Figure 2B, Supplementary Figure 2A).

293

294 **Transcriptome and WGCNA analysis of ESC exit from pluripotency with varying
295 β-catenin doses**

296 Next, we studied C1 ESCs exit from the ‘ground state’ of pluripotency, i.e., upon 2i/L
297 withdrawal, by RNA-sequencing; such monolayer differentiation protocol does not
298 induce a specific cell fate and is ideal to observe any β-catenin dependent
299 differentiation bias.

300 C1 ESCs cultured in 2i/L for 3 passages were treated for 48 hrs with saturating
301 concentrations of Doxy and TMP (100ng/mL and 10µM, respectively) to induce the
302 expression of the exogenous fusion protein (Figure 3A). Taking advantage of the
303 mCherry-tag for exogenous β-catenin overexpression, Doxy/TMP treated C1 ESCs
304 were sorted into two different subpopulations: C1 with Middle and High β-catenin
305 levels (hereafter called C1M and C1H samples, respectively; Figure 3A and
306 Supplementary Figure 3A). Cells were then seeded at 1.5×10^4 cells/cm² on gelatin-
307 coated plates and cultured in NDiff227 media±inducers for 4 days before being
308 transcriptionally profiled (see Methods for details; Figure 3A). Sequencing provided
309 snapshots of the C1, C1M and C1H samples transcriptome in pluripotent condition,
310 and of the differentiated counterparts (Day 4 samples) cultured in NDiff227 and DMSO
311 (i.e., upon Doxy/TMP withdrawal; hereafter called C1DMV and C1DHV), or in NDiff227
312 and TMP/Doxy (hereafter called C1DMDT and C1DHDT) during differentiation. The
313 C1 and C1D samples refer to cells treated only with TMP10µM in the pluripotent and
314 differentiated states, respectively.

315

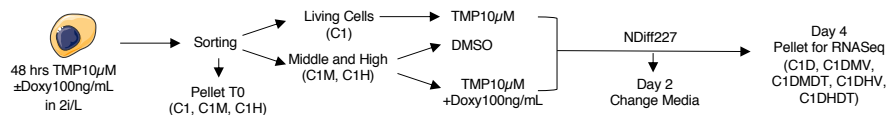
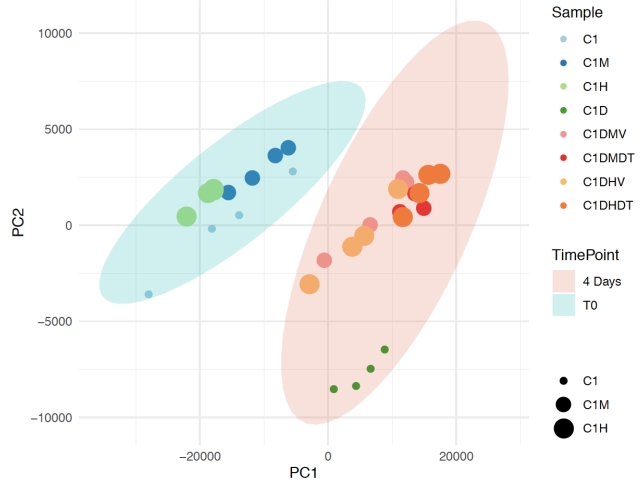
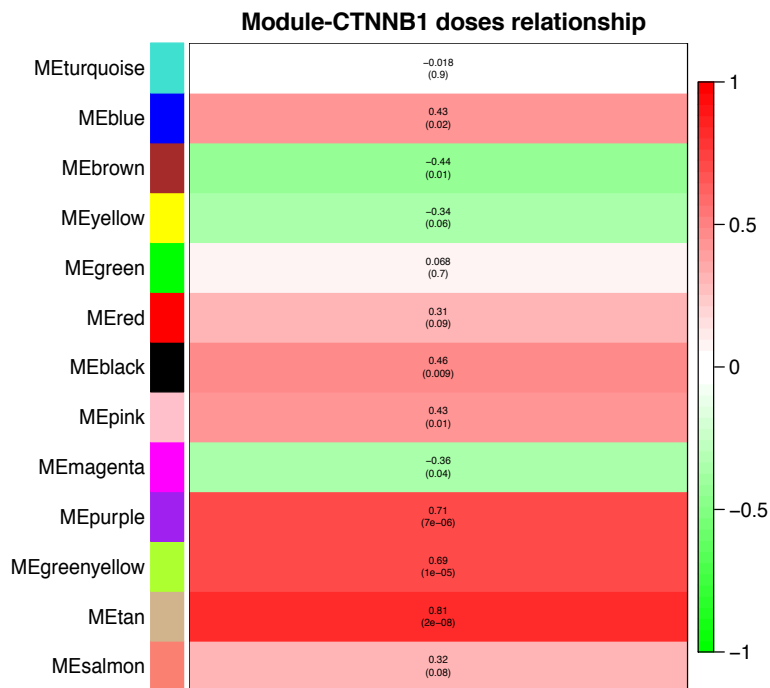
316 Principal Components Analysis (PCA, Figure 3B) showed three main clusters: one
317 group included C1, C1M and C1H in the ‘ground state’ of pluripotency, another group
318 included C1D ESCs and the final group contained all perturbed samples (C1DMV,
319 C1DHV, C1DMDT and C1DHDT) after 4 days of differentiation.

320

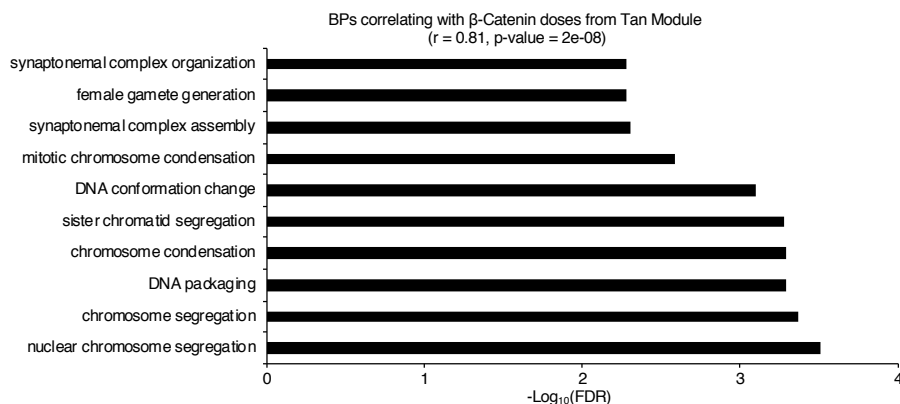
321 We next performed the Weighted Gene Correlation Network Analysis (WGCNA) to
322 pinpoint the processes associated with β-catenin perturbations. The WGCNA⁷⁰ is a
323 computational approach that allows the identification of gene modules based on their
324 correlation and network-derived topological properties. We applied the WGCNA to our

325 sequencing data and identified 13 different modules (Supplementary Figure 3B; see
326 Methods for details). We then defined the principal component of each module (i.e.,
327 eigenmodule, ME) and calculated the Pearson Correlation Coefficient (r) of each
328 eigenmodule with time (Supplementary Figure 3C) or β -catenin doses (Figure 3C).
329 Next, for each module, we performed a functional annotation analysis on the genes
330 with a module membership $|kME| \geq 0.8$ (Methods) to identify the biological processes
331 and pathways enriched (Supplementary Table 1), focusing the attention on the
332 modules having $r > 0.5$ and p -value < 0.05 with the examined traits (Figure 3C,
333 Supplementary Figure 3C, Methods).
334 We found four modules significantly correlating (i.e., Green $r = 0.92/p$ -value = 9e-14,
335 Blue $r = 0.82/p$ -value = 1e-08, Black $r = 0.67/p$ -value = 3e-05 and Brown $r = 0.57/p$ -
336 value = 7e-04; Supplementary Figure 3C, Supplementary Table 1) and three anti-
337 correlating (i.e., Turquoise $r = -0.99/p$ -value = 2e-24, yellow $r = -0.75/p$ -value = 1e-06
338 and Pink $r = -0.56/p$ -value = 8e-04; Supplementary Figure 3C, Supplementary Table
339 1) with time, meaning that these modules were regulated during the differentiation.
340 The biological processes (list of genes with a $kME > 0.8$; Supplementary Table 1)
341 related to these modules with a $FDR < 0.05$ showed an enrichment of genes involved
342 in translation, rRNA processing, ribosomal biogenesis and stem cell division
343 (Supplementary Figure 3D, F Supplementary Table 1, Green and Brown), protein
344 transport and processes associated with cellular respiration (Supplementary Figure
345 3E, Supplementary Table 1, Blue), positive regulation of growth, ncRNA processing
346 and neuronal tube formation and development (Supplementary Figure 3F,
347 Supplementary Table 1, Brown), regulation of tissue remodelling, embryonic and
348 forebrain development, stem cell population maintenance and cell homeostasis
349 (Supplementary Figure 3G, Supplementary Table 1, Turquoise), nuclear division and
350 meiosis and organelle fission (Supplementary Figure 3H, Supplementary Table 1,
351 Pink). For the pathway analysis, we found an enrichment in ribosome (Supplementary
352 Table 1, Green and Blue), Hedgehog signalling pathway (Supplementary Table 1,
353 Green), oxidative phosphorylation and diseases associated with oxidative stress
354 (Supplementary Table 1, Blue and Turquoise), cancer (Supplementary Table 1, Brown
355 and Turquoise) and regulation of the actin cytoskeleton (Supplementary Table 1,
356 Yellow). Of note, there were no significantly enriched BPs and/or pathways for the
357 genes from the Black, Yellow and Pink modules (Supplementary Table 1, Black,
358 Yellow and Pink).

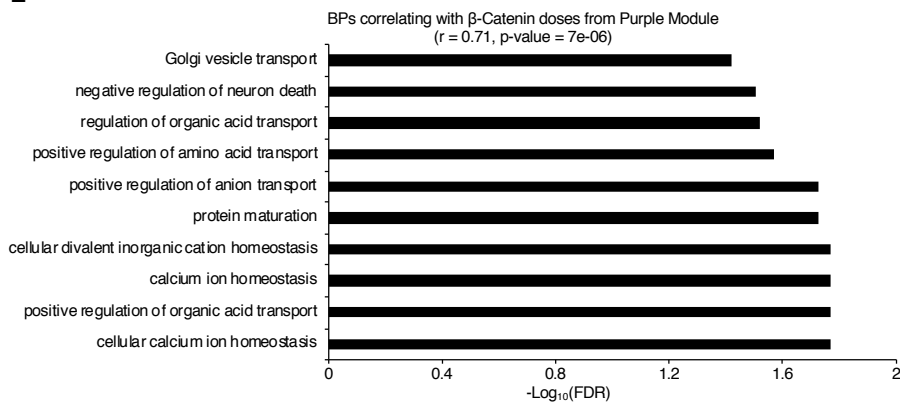
359 To gain more information about the effects of β -catenin at the exit from pluripotency,
360 we correlated the eigenmodule of each module with β -catenin doses (Figure 3C, see
361 Methods for details) and found three modules correlating with β -catenin doses (i.e.,
362 Tan $r = 0.81/p\text{-value} = 2\text{e-}8$, Purple $r = 0.71/p\text{-value} = 7\text{e-}6$ and Yellow/Green $r =$
363 $0.69/p\text{-value} = 1\text{e-}5$; Figure 3C, Supplementary Table 1). The biological processes (list
364 of genes with a kME > 0.8 ; Supplementary Table 1) corresponding to these modules
365 with a FDR < 0.05 showed enrichment in cell division (Figure 3D, Supplementary
366 Table 1, Tan), metabolism and negative regulation of neuronal death (Figure 3E,
367 Supplementary Table 1, Purple). Finally, the pathways analysis showed a significant
368 enrichment only in Lysosome and N-Glycan biosynthesis from the Purple module,
369 whereas pentose phosphate pathways and autophagy from the Green/Yellow
370 (Supplementary Table 1, Purple and GreenYellow).
371 Overall, the WGCNA analysis confirmed the expected major transcriptional and
372 metabolic changes associated with the exit from the pluripotent status, and confirmed
373 previously reported β -catenin functions on cell survival and proliferation³¹.

A**B****C**

D



E



375 **Figure 3. Transcriptome analysis of monolayer differentiation experiments upon
376 β -catenin perturbations and WGCNA of the genes correlating with β -catenin doses.**

377 **A** Experimental scheme of the monolayer differentiation protocol. 2i/L C1 ESCs were pre-
378 treated with TMP10 μ M and Doxy100ng/mL for 48 hrs; living cells were then sorted from the
379 Dapi negative fraction of TMP-treated cells (C1), whereas β -catenin overexpressing cells from
380 Doxy/TMP-treated samples were FACS-sorted from the mCherry fraction and divided into
381 Middle (C1M) and High (C1H) subpopulations. 1.5×10^4 cells/cm 2 from each individual
382 population were then seeded on gelatin in NDiff227 supplemented with DMSO or
383 TMP \pm Doxy100ng/mL. After 4 days of differentiation in NDiff227, cells were collected and
384 processed for the RNA sequencing. During the protocol, the media was changed, and the
385 drugs refreshed after 2 culture days. **B** Principal Component Analysis (PCA) of all samples;
386 the average of biological replica is shown. **C** Eigenmodules correlating with β -catenin doses;
387 the Pearson Correlation Coefficient (r) and relative p -value are shown. **D, E** Bar-chart of the
388 top-ten enriched biological processes (BP) with FDR < 0.05 from genes belonging to the Tan
389 (**D**) and Purple (**E**) WGCNA modules.

390

391 Next, to look at comparisons between specific pairs of samples, we performed a Gene
392 Ontology (GO) and Functional Annotation analysis on the differentially expressed

393 genes filtered for the false discovery rate (FDR < 0.05) and log fold change (logFC <
394 -2 or > 2; see Methods for details). To identify gene ontologies specific for each
395 experimental perturbation, we focused on the Biological Processes (BPs) enriched
396 only in one comparison (red bars in Figure 4A-D, Supplementary Figure 4A, B).
397 Starting from the pluripotent condition, when comparing C1M and C1H with C1 we
398 found that the first 10 biological processes with a FDR < 0.05 were mainly enriched in
399 cell cycles and metabolism (Supplementary Figure 4A, B, Supplementary Tables 2,
400 3). Interestingly, the genes exclusively upregulated in C1H compared to C1 were
401 related to tissue differentiation (i.e., eye morphogenesis and urogenital system
402 development) and DNA methylation involved in gamete generation (Supplementary
403 Figure 4B, Supplementary Table 3). Only a few signalling pathways were enriched in
404 C1M ESCs compared to the control cell line C1 (Supplementary Tables 2, 3). These
405 results, together with the PCA in Figure 3B, confirm previous observations about the
406 dispensable function β -catenin has in pluripotent culture conditions^{45-47,49} and suggest
407 a bias towards differentiation in C1H ESCs (Supplementary Figure 4B, Supplementary
408 Table 3).

409 We then analysed the genes differentially expressed at Day 4 upon β -catenin
410 perturbation as compared to C1D ESCs. Upregulated genes mostly contributed to the
411 BPs significantly enriched (Figure 4A-D, Supplementary Tables 4-7), while
412 downregulated genes only contributed to enrich a few processes, namely general
413 metabolic processes (e.g., regulation of transporter and cation channel activity) and
414 mesenchymal to epithelial transition (Figure 4A-D, Supplementary Tables 4-7). Genes
415 exclusively upregulated in the C1DMV vs C1D comparison belonged to the mesoderm
416 lineage (i.e., cardiovascular system development; Figure 4A and Supplementary
417 Table 4), while, in the C1DMDT vs C1D comparison, upregulated genes were enriched
418 for the endoderm lineage (i.e., urogenital system; Figure 4B and Supplementary Table
419 5). Nevertheless, mesoderm and endoderm lineages were represented in both
420 comparisons. GO performed on the C1DHV and C1DHDT comparisons with C1D
421 showed only a few differences in the enriched BPs, that indeed did not define a bias
422 toward a specific lineage (Figure 4C, D, Supplementary Tables 6, 7).

423 These results suggest that the major changes in the differentiation program initiated
424 upon 2i/L withdrawal are induced by moderate β -catenin doses and are influenced by
425 the timing of protein overexpression. The pathway enrichment analysis showed the
426 upregulation of protein metabolism in C1DMV and C1DHV (Supplementary Tables 4,

427 6), MAPK signalling pathway (Supplementary Table 4) in C1DMV, and ECM-receptor
428 interaction and PI3K-AKT signalling pathway in C1DHV (Supplementary Table 6).

429

430 To gauge insights into specific differentiation programs, we selected sets of markers
431 for naïve and general pluripotency, early post-implantation epiblast, ectoderm,
432 mesoderm, endoderm, germ cell and trophectoderm⁵¹, and clustered our samples
433 according to the expression of these gene sets.

434 Naïve pluripotency genes were downregulated during differentiation in all samples,
435 indicating the successful exit of cells from pluripotency (Figure 4E). Pluripotent C1M
436 and C1H samples clustered together (Figure 4E) although close to C1 ESCs, in
437 agreement with previous observations (Figure 3B). ESCs differentiated in presence of
438 DMSO (i.e., C1DMV and C1DHV; Figure 4E) clustered together, similarly to samples
439 differentiated in presence of Doxy and TMP (i.e., C1DMDT and C1DHDT, Figure 4E);
440 still, a large number of genes (e.g., Klf5, Tcl1, Klf2 and Nr0b1) showed a different
441 pattern among C1D, C1DMV, and C1DHV, discriminating ESCs with different β -
442 catenin doses (Figure 4E). These results support the hypothesis of a β -catenin-
443 dependent effect on transcriptional changes.

444 The clustering across samples was similar for general pluripotency markers (Figure
445 4F). In accordance with previous reports about the transition to primed pluripotency⁵⁵⁻
446 ⁵⁸, in the majority of differentiated samples Sox2 was downregulated and Utf1, Zfp281
447 and Lin28 were upregulated (Figure 4F). Moreover, almost all the genes were lower
448 in C1DMV, C1DMDT, C1DHV and C1DHDT as compared to C1D (exceptions were
449 Lin28a, higher in C1DHDT and Sox2, higher in C1DHV; Figure 4F), and showed
450 different behaviours in DMSO- (i.e., C1DMV and C1DHV; Figure 4F) vs Doxy/TMP-
451 treated samples (i.e., C1DMDT, C1DHDT; Figure 4F), confirming that the duration of
452 β -catenin overexpression has an influence on cell identity. Zfp281, Zic2 and Utf1
453 showed a similar pattern in β -catenin overexpressing cells as compared to C1D ESCs,
454 all being downregulated (Figure 4F). Zfp281 is a Zinc finger transcription factor
455 implicated in regulating stem cell pluripotency^{59,60}, and recently reported as a
456 bidirectional regulator of the ESC-EpiSC transition in cooperation with Zic2, another
457 zinc finger protein⁶¹. The undifferentiated embryonic cell transcription factor 1 (Utf1) is
458 expressed in ESCs and is involved in many aspects of gene expression control (e.g.,
459 transcription factor⁶² and epigenome organization^{63,64}), playing an important
460 regulatory role during the exit of ESCs from pluripotency^{63,64}. The concomitant

461 reduction of *Zfp281*, *Zic2* and *Urf1* suggests a global change in the chromatin
462 organization of β -catenin overexpressing ESCs en route to differentiation (Figure 4F).
463 Early post-implantation epiblast genes were mostly upregulated in primed ESCs
464 compared to the pluripotent condition with no evident differences across treatments in
465 naïve ESCs (Figure 4G). The exception was *Foxd3*, downregulated in both naïve and
466 primed β -catenin overexpressing cells as compared to the controls C1 and C1D ESCs
467 (Figure 4G). Interestingly, *Dnmt3a* levels, although similar at T0, were very different at
468 Day 4, with C1DMV/C1DHV and C1DMDT/C1DHDT showing 80% and 70% gene
469 expression reduction as compared to the control C1D, respectively (Figure 4G); also,
470 samples constantly exposed to Doxy/TMP (i.e., C1DMDT and C1DHDT) showed
471 higher *Dnmt3a* expression than DMSO-treated ESCs (i.e., C1DMV and C1DHV;
472 Figure 4G). Similar observations hold for *Dnmt3b*, where the reduction compared to
473 C1D was of about 60% for C1DMV/C1DHV and 10% for C1DMDT/C1DHDT (Figure
474 4G). *Dnmt3a*, *b* and *Foxd3* are DNA and chromatin remodelling factors, respectively;
475 *Dnmt* enzymes methylate genomic regions, whereas *Foxd3* reduces active and
476 enhances inactive histone marks by recruiting the Lysine-specific demethylase 1
477 (*Lsd1*)⁶⁵. The reduced expression of those genes in β -catenin overexpressing cells,
478 including the pluripotent markers *Utf1* discussed above, supports the hypothesis of
479 differentially methylated DNA.

480 We then screened for a large panel of lineage-priming factors. Clustering based on
481 the ectoderm lineage genes showed that pluripotent C1 and C1M are more similar
482 than C1H (Figure 4H); following 2i/L withdrawal, the clustering resembled those of
483 previous sets (Figure 4E-G), with C1DMV/C1DHV and C1DMDT/C1DHDT grouping
484 together (Figure 4H). Genes from this lineage had different and sometimes opposite
485 expression across samples, making difficult to identify a clear pattern associated with
486 β -catenin perturbations. Nevertheless, we distinguished two groups of genes: one
487 group (i.e., *Dlx3*, *Pou3f2*, *Otx1* and *Pou3f3*) was mainly downregulated during
488 differentiation, whereas the other group (i.e., *Nes*, *Ascl1*, *Cdh2* and *Pax6*) had the
489 opposite trend (Figure 4H).

490 When looking at mesoderm markers (Figure 4I), differentiated samples clustered
491 similarly to the previous data set; however, C1DMV/C1DHV were more similar to C1D
492 than in the previous comparisons (Figure 4E-H) and genes showed different
493 expression patterns across conditions. *Lhx1*, *Lefty1/2*, *Meox1*, *Hoxb1* and *Bmp4* were
494 mainly upregulated upon differentiation and no major differences were observed

495 across samples in pluripotent conditions. The exception in this group was Lhx1 that
496 was higher in β -catenin overexpressing cells depending on the timing of
497 overexpression (compare C1DMV/C1DHV with C1DMDT/C1DHDT in Figure 4I). In
498 contrast, genes such as Nodal, Kdr, Mixl1, Gsc, Foxf1 and Zic1 got downregulated
499 when exiting pluripotency and the levels across conditions were not significantly
500 changing (Figure 4I). Of note, although the behaviour of individual genes is hard to
501 interpret, C1D ESCs were very different from all differentiated samples with
502 perturbations of β -catenin, stressing the relevance of the latter for mesoderm
503 specification⁴⁶.

504 The endoderm lineage was the one most influenced by β -catenin perturbations: C1D
505 cells were unable to induce the expression of endoderm-related genes (compare C1
506 and C1D in Figure 4J), whereas in all perturbed ESCs their expression increased over
507 time. As previously observed (Figure 4E-I), samples clustered together based on the
508 duration of β -catenin overexpression rather than on its dose (i.e., C1DMV/C1DHV and
509 C1DMDT/C1DHDT, Figure 4J). Moreover, because of their impaired differentiation,
510 C1D clustered together with pluripotent samples (Figure 4J). The C1DHDT showed
511 the highest expression of the 50% of the endoderm-associated genes (namely, Cxcr4,
512 Gata4 and Sox7) as compared to all other differentiated samples (i.e., C1D, C1DMV,
513 C1DMDT and C1DHV). Slightly different was the behaviour of Cxcr4, that decreased
514 over time; however, its expression is indicative of definitive endoderm differentiation⁶⁶
515 that most probably is not happening in the short protocol we applied. These
516 observations, together with the incapability of C1D cells to embark differentiation
517 toward this lineage, strongly support previous knowledge about the β -catenin
518 requirement for endoderm organization^{46,67}.

519 In the analysis of the germ cell lineage markers, all genes showed a rather
520 heterogeneous expression pattern across samples (Figure 4K). Pluripotent C1M and
521 C1H clustered together and close to C1, and differentiated samples clustered based
522 on the duration of β -catenin perturbation (i.e., C1DMV/C1DHV and
523 C1DMDT/C1DHDT). Dazl, Prdm1 and Ddx4 showed a clearer pattern in pluripotent
524 conditions, being upregulated in C1M and C1H compared to C1 ESCs (Figure 4K).
525 Finally, when looking at trophectoderm markers, clustering showed similarity of C1
526 and C1M, as for the ectoderm and endoderm lineages (Figure 4H, J, respectively).
527 C1DMDT and C1DHDT were similar for the expression of trophectoderm genes,
528 whereas C1DMV was part of a different branch clustering with C1D; C1DHV was more

529 closely related to C1DMDT and C1DHDT (Figure 4L). Moreover, 90% of
530 trophectoderm genes got downregulated during differentiation (namely, Eomes, Elf3
531 and Cdx1) in all the conditions; the only exception was Cdx2 that was upregulated in
532 C1D, C1MDV and C1DMDT in comparison with the corresponding T0 (Figure 4L).
533 Eomes was recently reported to control the exit from pluripotency by acting on the
534 chromatin status⁶⁸; its behaviour in naïve C1M and C1H ESCs support the theory of a
535 different chromatin conformation in pluripotent β-catenin overexpressing cells (Figure
536 4L).

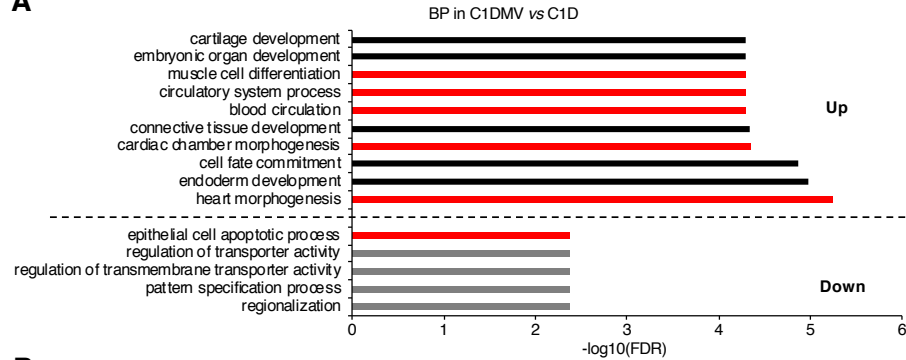
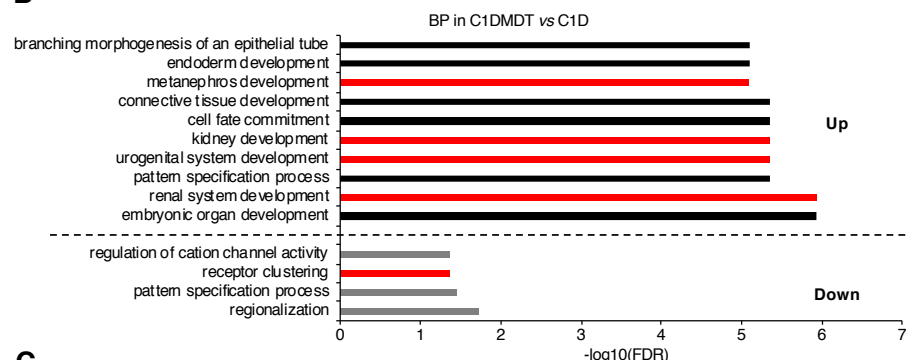
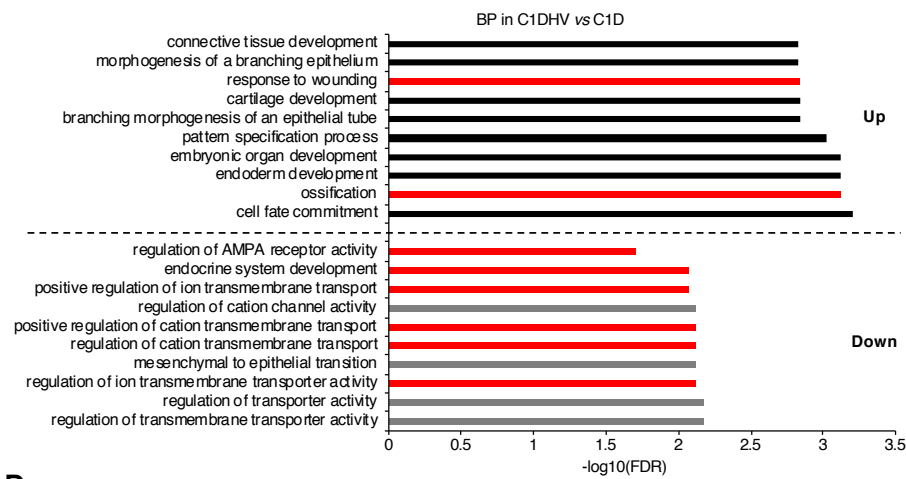
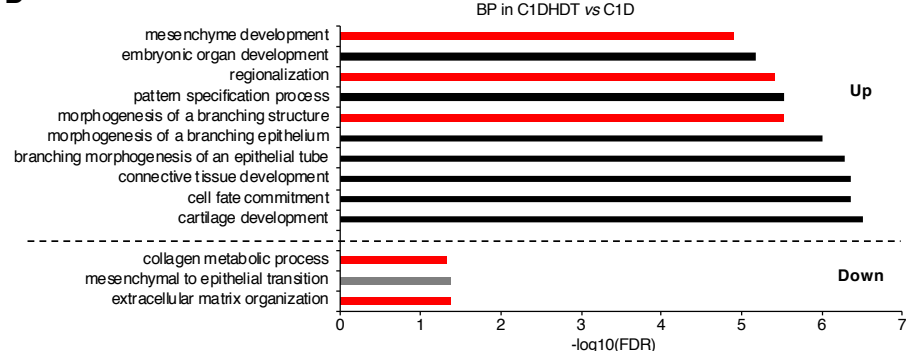
537

538 Accounting for the fact that ectoderm is a default lineage of the monolayer differentiation
539 protocol we applied⁶⁹, sequencing results suggest that β-catenin overexpression in a
540 knock-out background favours rescuing defects in differentiation towards endoderm
541 more than mesoderm. Indeed, mesodermal genes were mostly downregulated when
542 β-catenin was overexpressed, whereas endodermal genes were all upregulated as
543 compared to the control (Figure 4I, J). Moreover, we observed that lineage
544 differentiation was influenced by the duration of protein overexpression rather than the
545 dose. According to that, there was a transition from mesoderm to endoderm following
546 moderate but constant β-catenin overexpression (compare C1DMV and C1DMDT in
547 Figure 4A, B). Nevertheless, endoderm was an enriched gene ontology in all
548 considered comparisons (Figure 4A-D). Finally, the observed expression of
549 pluripotency markers Zfp281, Zic2 and Utf1, the early post-implantation markers
550 Dnmt3a-b and Foxd3 and the trophectoderm marker Eomes suggests a reorganization
551 of the epigenome in naïve C1M and C1H ESCs and upon monolayer differentiation of
552 C1DMV, C1DMDT, C1DHV and C1DHDT ESCs.

553

554

555

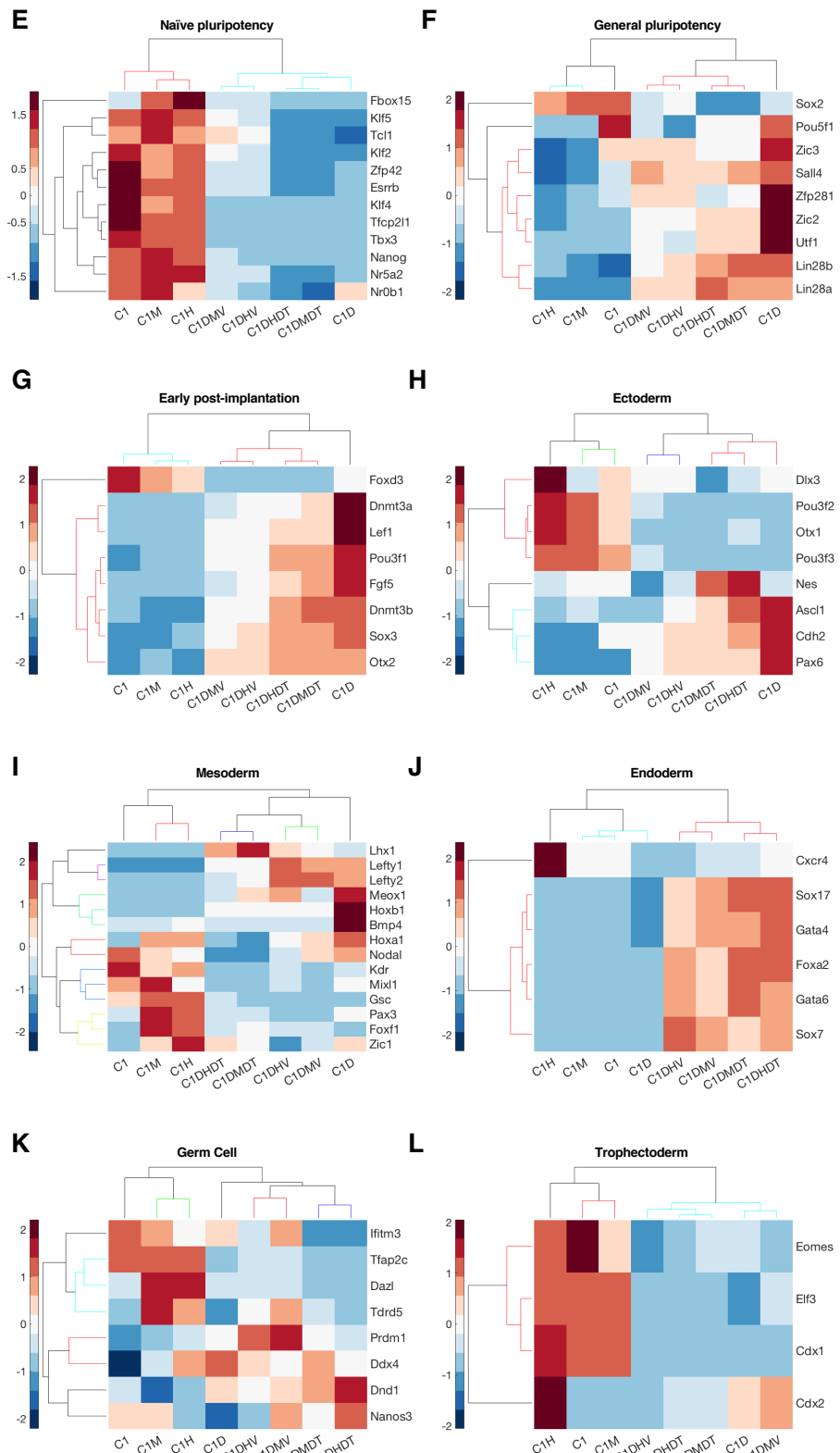
A**B****C****D**

556

557

558

559



560 **Figure 4. Gene ontology and clustergram of the differential expressed genes in control**
 561 **and perturbed ESCs.**

562 **A-D** Bar-chart of the top-ten enriched biological processes (BP) with FDR < 0.05 from
 563 differentially expressed genes in C1DMV (A), C1DMDT (B), C1DHV (C) and C1DHDT (D)
 564 compared to C1D ESCs. Black and grey bars represent upregulated and downregulated BPs,

565 respectively. In red bars, the BPs exclusively enriched in the indicated condition. **E-L**
566 Clustergram over heatmaps of Naïve (**E**) and general pluripotency (**H**), early post-implantation
567 (**G**), ectoderm (**H**), mesoderm (**I**), endoderm (**J**), germ cell (**K**) and trophectoderm (**L**) lineages
568 from pluripotent and differentiated ESCs expressing different β -catenin amount. Each column
569 is the average of 4 biological replicates.

570

571 **Discussion**

572 The role of the Wnt/ β -catenin pathway as a pluripotency gatekeeper has been matter
573 of many studies and debates^{30,42,48,71-74}; while modulation of the canonical Wnt
574 pathway has been extensively proved to be important for EpiSC *in vivo* derivation^{75,76},
575 self-renewal⁷⁷ and *in vitro* lineage differentiation⁷⁸⁻⁸⁰, its relevance for the exit from
576 pluripotency and for ESC-EpiSC direct transition have not been explored thoroughly.

577 In this work, we proved that genetic β -catenin manipulation or chemical perturbation
578 of the canonical Wnt pathway controls ESC fate at the exit from pluripotency.

579 Using two different cellular models, we found that moderate β -catenin doses in β -
580 catenin^{-/-} ESCs or its stabilization in wild-type ESCs increases the differentiation
581 efficiency of ESCs into EpiSCs, similarly to what was reported for EpiSCs self-
582 renewal²⁹. EpiSCs can be maintained in Chiron3 μ M/XAV2 μ M cultures, with self-
583 renewal regulated by both Axin2 and β -catenin²⁹; here we found that, in absence of
584 pre-activation of the canonical Wnt pathway, the Chiron3 μ M/XAV2 μ M treatment has
585 a better effect than Chiron3 μ M alone on ESC-EpiSC transition at the end of the
586 differentiation experiments (Day 3 and 4 in Figure 2B and Supplementary 2A), while
587 the opposite was observed in the early phases of the protocol (Day 1 and 2 in Figure
588 2B and Supplementary 2A). This could be explained by the fact that Axin2 expression
589 is β -catenin-dependent, and β -catenin stabilization gets induced by Chiron treatment;
590 therefore, the effect of XAV might be relevant only upon Axin2 stabilisation.
591 Alternatively, it might also suggest a switch in the effect of Chiron3 μ M/XAV2 μ M
592 stimulation in a specific moment during the differentiation process, probably when
593 ESCs start to acquire a more stable EpiSC identity (as in²⁹). Although both hypotheses
594 are in agreement with what was reported by Kim and colleagues²⁹, the first one seems
595 to be more plausible looking at the response in Ffg5 (Figure 1) and GFP expression
596 (Figure 2B, Supplementary Figure 2A), i.e., when a moderate activation of the Wnt/ β -
597 catenin pathway was induced. Indeed, both β -catenin^{-/-} exposed to a low concentration
598 of the input Doxy (i.e., TMP10 μ M _Doxy10ng/mL, “During Differentiation” in Figure

599 1D) and the dual reporter ESCs treated with Chiron1 μ M (i.e., C1 in Figure 2B) showed
600 the highest differentiation efficiency, suggesting that Chiron1 μ M treatment alone is
601 enough to keep β -catenin doses within a range that would instead require XAV
602 treatment if using higher doses of Chiron (i.e., 3 μ M), and that Chiron1 μ M is mimicking
603 the effect obtained by β -catenin genetic manipulation. Furthermore, XAV treatment in
604 combination with Chiron1 μ M reduced the percentage of differentiated cells at Day 1
605 (Figure 2B and Supplementary 2A); this could be due to the stoichiometry between β -
606 catenin, Ainx2 and the two inhibitors. We reason that, in Chiron1 μ M/XAV2 μ M, XAV is
607 in excess with respect to the amount of transcribed Axin2, therefore all the translated
608 protein gest stabilised, and the final effect is a strong inhibition of the signalling
609 pathway. Nevertheless, this effect might get attenuated with time, probably when a
610 balance between the drug and the target is achieved. This theory seems to be
611 supported by the behaviour of cells treated with Chiron1 μ M or Chiron3 μ M; the first
612 showed a GFP peak within the first 2 days followed by GFP stabilisation, while the
613 second showed the opposite trend (i.e., GFP reduction over time), suggesting that
614 prolonged β -catenin stabilization in FBS/L can impair ESCs differentiation towards
615 EpiSCs. These results pose the question of what would have happened if cells were
616 stimulated for longer with Chiron1 μ M. There are two possible scenarios; in the first,
617 EpiSCs, derived from ESCs, would self-renew in Chiron1 μ M as well as in
618 Chiron3 μ M/XAV2 μ M. In the second scenario, the transition from Chiron1 μ M to Chiron
619 3 μ M would be preferred for the maintenance of established EpiSCs. However, the
620 latter scenario would be in contrast with the results showed in²⁹, where it was proved
621 immediate differentiation or death of EpiSCs expanded in Chiron3 μ M \pm PD1 μ M. Of
622 note, the basal medium used in²⁹ for EpiSC self-renewal is based on minimal essential
623 medium (GMEM) supplemented with 10% FBS²⁹, therefore differences might be
624 expected. Finally, we found that 2i/L pre-cultured ESCs better differentiate into
625 EpiSCs, regardless of further modulation of the pathway during differentiation. It has
626 been shown that, during the differentiation process, ESCs downregulate Oct4
627 expression and undergo a temporary cell cycle arrest⁵⁴; when differentiation has been
628 accomplished, Oct4 levels and cell cycle progression are restored to support the clonal
629 expansion of the EpiSC population. However, rare Oct4-/Cdx2+ cells might appear
630 during the initial phase of the differentiation process; this cellular fraction does not
631 respond to the cell cycle arrest, and therefore has a proliferative advantage⁵⁴. The
632 simultaneous elimination of differentiating incompetent cells (i.e., Oct4-/Cdx2+) and

633 the re-established proliferation of differentiated cells (i.e., Oct4+/Cdx2-) ensure a
634 homogenous population of EpiSCs⁵⁴.

635 We and others reported a reduced proliferation rate of ESCs stimulated with Chiron
636 both in FBS/L³¹ and 2i/L¹³. In agreement with these observations, we hypothesise that
637 Chiron treatment might reduce the proliferation of Oct4-/Cdx2+ cells, establishing a
638 balance between differentiating competent (i.e., Oct4-/Cdx2-) and incompetent (i.e.,
639 Oct4-/Cdx2+) cells. The 2i/L pre-culture might additionally homogenise the expression
640 of various genes, including Oct4⁸¹ and reduce the appearance of Cdx2+ cells.

641 Overall, these results confirm the effect β -catenin has on preparing cells to
642 appropriately respond to the differentiation stimuli and suggest that both the duration
643 and the dose of β -catenin overexpression control cell differentiation *in vitro*. Moreover,
644 they enabled us to define an improved protocol for EpiSCs derivation *in vitro*, based
645 on NDiff227 and Chiron1 μ M.

646 RNA sequencing performed in ESCs during the exit from the naïve ‘ground state’ of
647 pluripotency⁵¹ showed that, in β -catenin overexpressing cells (in particular in C1DMV),
648 Dnmt3a and b had an expression pattern similar to the one observed in Rex1-high
649 ESCs differentiated using a similar protocol⁵¹, indicating that moderate β -catenin
650 overexpression in naïve ESCs influences DNA methylation associated with the exit
651 from pluripotency. Interestingly, we observed a significant upregulation of endodermal
652 genes in β -catenin overexpressing cells, indicating a requirement of β -catenin for this
653 specific fate. This phenotype was previously reported in the β -catenin null cell line
654 generated by Lyashenko and colleagues⁴⁶, where the defect in endoderm lineage
655 differentiation was rescued by overexpressing both wild-type or transcriptional
656 incompetent β -catenin⁴⁶; in contrast, mesoderm and ectoderm induction seemed to
657 not require β -catenin⁴⁶. With our approach that enables dose- and time-controlled β -
658 catenin overexpression, we were able to define the amount of protein and the optimal
659 window of overexpression to facilitate mesoderm (i.e., C1DMV; Figure 4A,
660 Supplementary Table 4) or endoderm (i.e., C1DMDT; Figure 4B, Supplementary Table
661 5) differentiation, and confirmed that the ectoderm lineage is not affected by β -catenin
662 loss and therefore is not influenced by its overexpression.

663 In the future, it will be of great interest to use our inducible system to interrogate the
664 effect of more complex β -catenin dynamics on stem-cell identity and to further
665 investigate the role of the β -catenin transcriptional activity in pluripotent and
666 differentiated cells of both murine and human origin.

667

668 **Authors Contributions**

669 E.P. designed and performed experiments; M.F. and G.G. performed the WGNCA
670 analysis; M.F. performed the GO; R.D.C. performed the Differential Expression
671 analysis; E.P., and L.M. analysed data; E.P., M.F., R.D.C. and L.M. wrote the paper;
672 D.d.B. supervised the bioinformatics analysis; L.M. supervised the entire project.

673

674 **Acknowledgements**

675 We thank Dr Robert Blelloch for the *miR-290-mCherry/miR-302-eGFP* ESC line; Dr
676 Andre Hermann and Dr Lorena Sueiro Ballesteros (Flow Cytometry Facility, University
677 of Bristol), Dr Mark Jepson and Alan Leard (Wolfson Imaging Facility, University of
678 Bristol) and the Next Generation Sequencing Core (TIGEM, Naples) for their support.
679 This work was funded by Medical Research Council (grant MR/N021444/1) to L.M.,
680 by the Engineering and Physical Sciences Research Council (grants EP/R041695/1
681 and EP/S01876X/1 to L.M.), EC funding H2020 (FET OPEN 766840-COSY-BIO) to
682 L.M., BrisSynBio, a BBSRC/EPSRC Synthetic Biology Research Centre
683 (BB/L01386X/1) to L.M, STAR-University of Naples Federico II grant to G.G. and
684 Fondazione Telethon grant to D.d.B.

685

686 **Methods**

687 **Cell line derivation**

688 C1 cell lines were previously derived in⁴⁹ by a double lentiviral infection of β -catenin^{-/-}
689 ESCs⁴⁵ with the EF1a-rtTA (Neomycin) plasmid followed by the pLVX_TrE3G-
690 DDmCherry β -catenin^{S33Y}(Puromycin). Cells were selected with Neomycin after the
691 first round and with Puromycin after the last infection. The dual reporter ESCs were a
692 gift from Dr Blelloch⁵³.

693 ESCs were cultured on gelatin-coated dishes in Dulbecco's modified Eagle's medium
694 (DMEM) supplemented with 15% fetal bovine serum (FBS, Sigma), 1 x nonessential
695 amino acids, 1 x GlutaMax, 1 x 2-mercaptoethanol and 1000 U/mL LIF (Peprotech). To
696 note, that for the 2i/L culture, cells were kept for 3 passages (around 1 week) in serum-
697 free NDiff227-based media supplemented with 1000 U/mL LIF, 3 μ M of the GSK-3 α / β
698 inhibitor Chiron-99021 (Selleck, S1263) and 1 μ M of the MEK inhibitor PD0325901
699 (Selleck, S1036).

700

701 **Epiblast Differentiation**

702 For EpiSC derivation *in vitro*, FBS/L and 2i/L 1.5×10^4 cells/cm² were seeded on
703 10µg/mL Fibronectin-coated 12-well plates in NDiff227 (Takara, Y40002) and,
704 according to the experiment, stimulated with DMSO, TMP10µM (Sigma, T7883), Doxy
705 10-100ng/mL (Sigma, D9891), human ActivinA 10ng/mL (Peptrotech, 120-14E),
706 human FGF2 10ng/mL (Peptrotech, 100-18B) Chiron1-3µM and the XAV939 2µM
707 (Sigma, 575545) for 4 days with the media and drugs refreshed after the first 2 culture
708 days (Figures 1B, C and 2A).

709

710 **Monolayer differentiation**

711 Sorted C1, C1M and C1H ESCs were plated at 1.5×10^4 cells/cm² on gelatin-coated
712 12-well plates in plain NDiff227 and stimulated with DMSO or TMP10µM±Doxo10-
713 100ng/mL for 4 days with the media and drugs refreshed after the first 2 culture days
714 (Figure 3A).

715

716 **Drugs pre-treatment**

717 Some experimental conditions required pre-treatment of cells. For β-catenin
718 overexpression in Figure 1C, C1 ESCs were stimulated for 48 hrs with TMP10µM and
719 Doxo10-100ng/mL before the EpiSC differentiation, whereas for pre-activation of the
720 canonical Wnt pathway in Figure 2A, C-E and Supplementary Figure 2B-D, dual
721 reported ESCs were exposed to Chiron1-3µM (Figure 2C, Supplementary Figure 2B
722 and Figure 2D, Supplementary Figure 2C, respectively) for 48 hrs or cultured for 3
723 passages in 2i/L (Figure 2E, Supplementary Figure 2D), before the differentiation.

724

725 **Flow cytometry analysis**

726 ESCs from a 12-well plate were washed with sterile Phosphate-Buffered Saline (PBS,
727 Gibco), incubated with 80 µL of trypsin for 2–3' at room temperature and collected with
728 120 µL of PBS 2% FBS containing DAPI as cell viability marker. Cell suspension was
729 analysed using the BD LSR Fortessa and 10,000 living cells were recorded for each
730 sample. The % of GFP positive cells was calculated over living cells, gated as DAPI
731 negative, using the FlowJo V10 software.

732

733 **Flow activated cell sorting (FACS)**

734 ESCs were washed with sterile phosphate-buffered saline (PBS, Gibco), trypsinised
735 for 2-3' at room temperature and centrifuged at 1000 × g for 5'. Pelleted cells were
736 resuspended in 500 µL of plain NDiff227 media supplemented with DAPI. The
737 mCherry positive fraction was sorted from DAPI negative using the BD Influx high-
738 speed 16-parameter fluorescence activated cell sorter.

739

740 **qPCR**

741 For quantitative PCR, the total RNA, extracted from cells using the RNeasy kit
742 (Qiagen), was retrotranscribed (Thermo Fischer, RevertAid Reverse Transcriptase
743 EP0441) and the cDNA used as template for each qPCR reaction in a 15 µL reaction
744 volume. iTaq Universal SYBR Green Supermix (1725120, Bio-Rad) was used with the
745 Qiagen Rotor-Gene System. To eliminate the contamination from genomic DNA, the
746 RNeasy Plus Mini Kit (Qiagen, 74134) was used to purify the total RNA used for the
747 RNA Sequencing. The primers used were: Actin-Fwd:
748 ACGTTGACATCCGTAAAGACCT, Actin-Rev: GCAGTAATCTCCTTCTGCATCC;
749 Fgf5-Fwd: AAAACCTGGTGCACCCCTAGA, Fgf5-Rev:
750 CATCACATTCCCGAATTAAGC).

751

752 **Time-lapse experiments**

753 1.5×10⁴ cells were seeded on 10µg/mL fibronectin-coated µ-Slide 8 Well Glass Bottom
754 (Ibidi, 80827) and imaged with a Leica DMI6000 inverted epifluorescence microscope
755 equipped with the Photometrics Prime 95B sCMOS camera (1200x1200 11µm pixels,
756 8,12 bit or 16 bit, 70 fps full frame) and an environmental control chamber (Solent)
757 for long- term temperature control and CO₂ enrichment. The Adaptive Focus Control
758 (AFC) ensures focus is maintained during multiple acquisition cycles. Images were
759 acquired from two channels (phase contrast and green fluorescence) with a 20X
760 objective every 60min for 71 hrs. ImageJ version: 2.0.0-rc-69/1.52p was used to
761 improve the GFP signal, apply a Gaussian blur filter (Sigma radius 2) and combine
762 channels.

763

764 **QuantSeq 3' RNA sequencing library preparation.**

765 Preparation of libraries was performed with a total of 100ng of RNA from each sample
766 using QuantSeq 3'mRNA-Seq Library prep kit (Lexogen, Vienna, Austria) according
767 to manufacturer's instructions. Total RNA was quantified using the Qubit 2.0

768 fluorimetric Assay (Thermo Fisher Scientific). Libraries were prepared from 100ng of
769 total RNA using the QuantSeq 3' mRNA-Seq Library Prep Kit FWD for Illumina
770 (Lexogen GmbH). Quality of libraries was assessed by using screen tape High
771 sensitivity DNA D1000 (Agilent Technologies). Libraries were sequenced on a
772 NovaSeq 6000 sequencing system using an S1, 100 cycles flow cell (Illumina Inc.).
773 Amplified fragmented cDNA of 300 bp in size were sequenced in single-end mode with
774 a read length of 100 bp.

775 Illumina novaSeq base call (BCL) files are converted in fastq file through bcl2fastq
776 [http://emea.support.illumina.com/content/dam/illuminasupport/documents/documentation/software_documentation/bcl2fastq/bcl2fastq2-v2-20-software-guide-15051736-03.pdf] (version v2.20.0.422).
777

778

779 **QuantSeq 3' RNA sequencing data processing and analysis.**

780 For analysis, sequence reads were trimmed using bbduk software
781 (<https://jgi.doe.gov/data-and-tools/bbtools/bb-tools-user-guide/usage-guide/>) (bbmap
782 suite 37.31) to remove adapter sequences, poly-A tails and low-quality end bases
783 (regions with average quality below 6). Alignment was performed with STAR 2.6.0a3⁸²
784 on mm10 reference assembly obtained from cellRanger website
785 (https://support.10xgenomics.com/single-cell-gene-expression/software/release-notes/build#mm10_3.0.0; Ensembl assembly release 93). Expression levels of genes
786 were determined with htseq-count⁸³ using Gencode/Ensembl gene model. We have
787 filtered out all genes having < 1 cpm in less than n_min samples and Perc MM reads
788 > 20% simultaneously. Differential expression analysis was performed using edgeR⁸⁴,
789 a statistical package based on generalized linear models, suitable for multifactorial
790 experiments. The threshold for statistical significance chosen was False Discovery
791 Rate (FDR) < 0.05 (GSE148879). The lists of differentially expressed genes (DEGs),
792 for each comparison, with a threshold of logFC > 2 for the induced and logFC < -2 for
793 the inhibited transcripts (Supplementary Tables 2-7) were used for the Functional
794 Annotation analysis.
795

796 The data were deposited in GEO with the accession number GSE148879.
797

798

799 **Weighted Gene Correlation Network Analysis (WGCNA)**

800 Quant-seq 3' mRNA data of 32 samples was used to construct a gene co-expression
801 network by applying Weighted Gene Correlation Network Analysis (WGCNA)⁷⁰ from

802 the WGCNA package in the R statistical environment version 3.6. Briefly, we first
803 computed the Pearson correlation coefficient among all pairs of expressed genes and
804 then an appropriate value of the soft-thresholding power ($\beta=6$) giving a scale-free
805 topology fitting index (R^2) ≥ 0.85 was selected to build the weighted adjacency matrix.
806 The weighted adjacency matrix was further transformed into a topological overlap
807 matrix (TOM)⁸⁵ and the resulting dissimilarity matrix used for hierarchical clustering.
808 Gene modules were finally identified by cutting the hierarchical dendrogram with the
809 dynamic tree cut algorithm from dynamicTreeCut package in R⁸⁶ statistical
810 environment with standard parameters, except for cutHeight we set equal to 0.25 and
811 deepSplit we set equal to 1. The value of deepSplit parameter was selected after
812 performing a cluster stability analysis. Briefly, for each possible value of deepSplit
813 parameter (i.e., 0, 1, 2, 3 or 4), modules were identified for both the full dataset and
814 50 resampled datasets. Then, the clustering solution obtained for the full dataset was
815 compared with each resampled solution by mean of Adjusted Rand Index (ARI)⁸⁷. The
816 solution giving the highest average ARI was used for the clustering analysis as
817 described above. Finally, to identify which clusters were correlated with β -catenin
818 expression doses or differentiation time we correlated the first principal component of
819 each gene module (i.e., the eigenmodule) with the traits of interest. The eigenmodule
820 can be considered as a “signature” of the module gene expression. Modules correlated
821 with the traits with a p-value < 0.01 were considered statistically significant and used
822 for further analyses.

823

824 **Functional Annotation Analysis**

825 Differentially expressed genes (either $\log FC > 2$ or $\log FC < -2$) and module “hubs”
826 having high module membership (also known as $|KME| > 0.8$) within the module were
827 analysed for the enrichment in GO Biological Processes⁸⁸ and KEGG Pathways⁸⁹ via
828 the clusterProfiler package in R statistical environment⁹⁰. The threshold for statistical
829 significance was $FDR < 0.05$, the top-ten BPs were represented as $-\log_{10}$ (FDR;
830 Figure 3D-E, Supplementary Figure 3D-H, and Figure 4A-D, Supplementary Figure
831 4A, B).

832

833 **Statistical analysis**

834 Differences between samples were analysed by two-tailed unpaired t test and one-
835 way ANOVA using Matlab (MathworksMatlab R2019a, update 9.6.0.1307630). A p-
836 value lower than 0.05 was considered statistically significant.
837 Clustergram over heatmaps were generated using the clustergram function in Matlab
838 (MathworksMatlab R2019a, update 9.6.0.1307630) that applies the Euclidean
839 distance metric and average linkage. The data have been standardized across all
840 samples for each gene and have 0 as mean and 1 as standard deviation.

841

842 **References**

843

- 844 1 Evans, M. J. & Kaufman, M. H. Establishment in culture of pluripotential cells
845 from mouse embryos. *Nature* **292**, 154-156, doi:10.1038/292154a0 (1981).
- 846 2 Martin, G. R. Isolation of a pluripotent cell line from early mouse embryos
847 cultured in medium conditioned by teratocarcinoma stem cells. *Proc Natl Acad
848 Sci U S A* **78**, 7634-7638, doi:10.1073/pnas.78.12.7634 (1981).
- 849 3 Ying, Q. L., Wray, J., Nichols, J., Batlle-Morera, L., Doble, B., Woodgett, J.,
850 Cohen, P. & Smith, A. The ground state of embryonic stem cell self-renewal.
851 *Nature* **453**, 519-523, doi:10.1038/nature06968 (2008).
- 852 4 Brook, F. A. & Gardner, R. L. The origin and efficient derivation of embryonic
853 stem cells in the mouse. *Proc Natl Acad Sci U S A* **94**, 5709-5712,
854 doi:10.1073/pnas.94.11.5709 (1997).
- 855 5 Williams, R. L., Hilton, D. J., Pease, S., Willson, T. A., Stewart, C. L., Gearing,
856 D. P., Wagner, E. F., Metcalf, D., Nicola, N. A. & Gough, N. M. Myeloid
857 leukaemia inhibitory factor maintains the developmental potential of embryonic
858 stem cells. *Nature* **336**, 684-687, doi:10.1038/336684a0 (1988).
- 859 6 Smith, A. G., Heath, J. K., Donaldson, D. D., Wong, G. G., Moreau, J., Stahl,
860 M. & Rogers, D. Inhibition of pluripotential embryonic stem cell differentiation
861 by purified polypeptides. *Nature* **336**, 688-690, doi:10.1038/336688a0 (1988).
- 862 7 Ying, Q. L., Nichols, J., Chambers, I. & Smith, A. BMP induction of Id proteins
863 suppresses differentiation and sustains embryonic stem cell self-renewal in
864 collaboration with STAT3. *Cell* **115**, 281-292, doi:10.1016/s0092-
865 8674(03)00847-x (2003).

866 8 Niwa, H., Burdon, T., Chambers, I. & Smith, A. Self-renewal of pluripotent
867 embryonic stem cells is mediated via activation of STAT3. *Genes Dev* **12**, 2048-
868 2060, doi:10.1101/gad.12.13.2048 (1998).

869 9 Matsuda, T., Nakamura, T., Nakao, K., Arai, T., Katsuki, M., Heike, T. & Yokota,
870 T. STAT3 activation is sufficient to maintain an undifferentiated state of mouse
871 embryonic stem cells. *EMBO J* **18**, 4261-4269, doi:10.1093/emboj/18.15.4261
872 (1999).

873 10 Marucci, L., Pedone, E., Di Vicino, U., Sanuy-Escribano, B., Isalan, M. &
874 Cosma, M. P. beta-catenin fluctuates in mouse ESCs and is essential for
875 Nanog-mediated reprogramming of somatic cells to pluripotency. *Cell Rep* **8**,
876 1686-1696, doi:10.1016/j.celrep.2014.08.011 (2014).

877 11 Boroviak, T., Loos, R., Lombard, P., Okahara, J., Behr, R., Sasaki, E., Nichols,
878 J., Smith, A. & Bertone, P. Lineage-Specific Profiling Delineates the Emergence
879 and Progression of Naive Pluripotency in Mammalian Embryogenesis. *Dev Cell*
880 **35**, 366-382, doi:10.1016/j.devcel.2015.10.011 (2015).

881 12 Marks, H., Kalkan, T., Menafra, R., Denissov, S., Jones, K., Hofemeister, H.,
882 Nichols, J., Kranz, A., Stewart, A. F., Smith, A. & Stunnenberg, H. G. The
883 transcriptional and epigenomic foundations of ground state pluripotency. *Cell*
884 **149**, 590-604, doi:10.1016/j.cell.2012.03.026 (2012).

885 13 Godwin, S., Ward, D., Pedone, E., Homer, M., Fletcher, A. G. & Marucci, L. An
886 extended model for culture-dependent heterogenous gene expression and
887 proliferation dynamics in mouse embryonic stem cells. *NPJ Syst Biol Appl* **3**,
888 19, doi:10.1038/s41540-017-0020-5 (2017).

889 14 Ghimire, S., Van der Jeught, M., Neupane, J., Roost, M. S., Anckaert, J.,
890 Popovic, M., Van Nieuwerburgh, F., Mestdagh, P., Vandesompele, J., Deforce,
891 D., Menten, B., Chuva de Sousa Lopes, S., De Sutter, P. & Heindryckx, B.
892 Comparative analysis of naive, primed and ground state pluripotency in mouse
893 embryonic stem cells originating from the same genetic background. *Sci Rep*
894 **8**, 5884, doi:10.1038/s41598-018-24051-5 (2018).

895 15 Ficz, G., Hore, T. A., Santos, F., Lee, H. J., Dean, W., Arand, J., Krueger, F.,
896 Oxley, D., Paul, Y. L., Walter, J., Cook, S. J., Andrews, S., Branco, M. R. &
897 Reik, W. FGF signaling inhibition in ESCs drives rapid genome-wide
898 demethylation to the epigenetic ground state of pluripotency. *Cell Stem Cell* **13**,
899 351-359, doi:10.1016/j.stem.2013.06.004 (2013).

900 16 Habibi, E., Brinkman, A. B., Arand, J., Kroese, L. I., Kerstens, H. H., Matarese, F., Lepikhov, K., Gut, M., Brun-Heath, I., Hubner, N. C., Benedetti, R., Altucci, L., Jansen, J. H., Walter, J., Gut, I. G., Marks, H. & Stunnenberg, H. G. Whole-genome bisulfite sequencing of two distinct interconvertible DNA methylomes of mouse embryonic stem cells. *Cell Stem Cell* **13**, 360-369, doi:10.1016/j.stem.2013.06.002 (2013).

906 17 Leitch, H. G., McEwen, K. R., Turp, A., Encheva, V., Carroll, T., Grbole, N., Mansfield, W., Nashun, B., Knezovich, J. G., Smith, A., Surani, M. A. & Hajkova, P. Naive pluripotency is associated with global DNA hypomethylation. *Nat Struct Mol Biol* **20**, 311-316, doi:10.1038/nsmb.2510 (2013).

910 18 Nichols, J. & Smith, A. Pluripotency in the embryo and in culture. *Cold Spring Harb Perspect Biol* **4**, a008128, doi:10.1101/cshperspect.a008128 (2012).

912 19 Alexandrova, S., Kalkan, T., Humphreys, P., Riddell, A., Scognamiglio, R., Trumpp, A. & Nichols, J. Selection and dynamics of embryonic stem cell integration into early mouse embryos. *Development* **143**, 24-34, doi:10.1242/dev.124602 (2016).

916 20 Tesar, P. J., Chenoweth, J. G., Brook, F. A., Davies, T. J., Evans, E. P., Mack, D. L., Gardner, R. L. & McKay, R. D. New cell lines from mouse epiblast share defining features with human embryonic stem cells. *Nature* **448**, 196-199, doi:10.1038/nature05972 (2007).

920 21 Brons, I. G., Smithers, L. E., Trotter, M. W., Rugg-Gunn, P., Sun, B., Chuva de Sousa Lopes, S. M., Howlett, S. K., Clarkson, A., Ahrlund-Richter, L., Pedersen, R. A. & Vallier, L. Derivation of pluripotent epiblast stem cells from mammalian embryos. *Nature* **448**, 191-195, doi:10.1038/nature05950 (2007).

924 22 Han, D. W., Tapia, N., Joo, J. Y., Greber, B., Arauzo-Bravo, M. J., Bernemann, C., Ko, K., Wu, G., Stehling, M., Do, J. T. & Scholer, H. R. Epiblast stem cell subpopulations represent mouse embryos of distinct pregastrulation stages. *Cell* **143**, 617-627, doi:10.1016/j.cell.2010.10.015 (2010).

928 23 Stavridis, M. P., Lunn, J. S., Collins, B. J. & Storey, K. G. A discrete period of FGF-induced Erk1/2 signalling is required for vertebrate neural specification. *Development* **134**, 2889-2894, doi:10.1242/dev.02858 (2007).

931 24 Kunath, T., Saba-El-Leil, M. K., Almousailleakh, M., Wray, J., Meloche, S. & Smith, A. FGF stimulation of the Erk1/2 signalling cascade triggers transition of

933 pluripotent embryonic stem cells from self-renewal to lineage commitment.
934 *Development* **134**, 2895-2902, doi:10.1242/dev.02880 (2007).

935 25 Greber, B., Wu, G., Bernemann, C., Joo, J. Y., Han, D. W., Ko, K., Tapia, N.,
936 Sabour, D., Sterneckert, J., Tesar, P. & Scholer, H. R. Conserved and divergent
937 roles of FGF signaling in mouse epiblast stem cells and human embryonic stem
938 cells. *Cell Stem Cell* **6**, 215-226, doi:10.1016/j.stem.2010.01.003 (2010).

939 26 Guo, G., Yang, J., Nichols, J., Hall, J. S., Eyres, I., Mansfield, W. & Smith, A.
940 Klf4 reverts developmentally programmed restriction of ground state
941 pluripotency. *Development* **136**, 1063-1069, doi:10.1242/dev.030957 (2009).

942 27 Johansson, B. M. & Wiles, M. V. Evidence for involvement of activin A and bone
943 morphogenetic protein 4 in mammalian mesoderm and hematopoietic
944 development. *Mol Cell Biol* **15**, 141-151, doi:10.1128/mcb.15.1.141 (1995).

945 28 Yao, S., Chen, S., Clark, J., Hao, E., Beattie, G. M., Hayek, A. & Ding, S. Long-
946 term self-renewal and directed differentiation of human embryonic stem cells in
947 chemically defined conditions. *Proc Natl Acad Sci U S A* **103**, 6907-6912,
948 doi:10.1073/pnas.0602280103 (2006).

949 29 Kim, H., Wu, J., Ye, S., Tai, C. I., Zhou, X., Yan, H., Li, P., Pera, M. & Ying, Q.
950 L. Modulation of beta-catenin function maintains mouse epiblast stem cell and
951 human embryonic stem cell self-renewal. *Nat Commun* **4**, 2403,
952 doi:10.1038/ncomms3403 (2013).

953 30 Sato, N., Meijer, L., Skaltsounis, L., Greengard, P. & Brivanlou, A. H.
954 Maintenance of pluripotency in human and mouse embryonic stem cells
955 through activation of Wnt signaling by a pharmacological GSK-3-specific
956 inhibitor. *Nat Med* **10**, 55-63, doi:10.1038/nm979 (2004).

957 31 De Jaime-Soguero, A., Aulicino, F., Ertaylan, G., Griego, A., Cerrato, A.,
958 Tallam, A., Del Sol, A., Cosma, M. P. & Lluis, F. Wnt/Tcf1 pathway restricts
959 embryonic stem cell cycle through activation of the Ink4/Arf locus. *PLoS Genet*
960 **13**, e1006682, doi:10.1371/journal.pgen.1006682 (2017).

961 32 Stamos, J. L. & Weis, W. I. The beta-catenin destruction complex. *Cold Spring
962 Harb Perspect Biol* **5**, a007898, doi:10.1101/cshperspect.a007898 (2013).

963 33 Jho, E. H., Zhang, T., Domon, C., Joo, C. K., Freund, J. N. & Costantini, F.
964 Wnt/beta-catenin/Tcf signaling induces the transcription of Axin2, a negative
965 regulator of the signaling pathway. *Mol Cell Biol* **22**, 1172-1183,
966 doi:10.1128/mcb.22.4.1172-1183.2002 (2002).

967 34 Chia, I. V. & Costantini, F. Mouse axin and axin2/conductin proteins are
968 functionally equivalent in vivo. *Mol Cell Biol* **25**, 4371-4376,
969 doi:10.1128/MCB.25.11.4371-4376.2005 (2005).

970 35 Leung, J. Y., Kolligs, F. T., Wu, R., Zhai, Y., Kuick, R., Hanash, S., Cho, K. R.
971 & Fearon, E. R. Activation of AXIN2 expression by beta-catenin-T cell factor. A
972 feedback repressor pathway regulating Wnt signaling. *J Biol Chem* **277**, 21657-
973 21665, doi:10.1074/jbc.M200139200 (2002).

974 36 Glinka, A., Wu, W., Delius, H., Monaghan, A. P., Blumenstock, C. & Niehrs, C.
975 Dickkopf-1 is a member of a new family of secreted proteins and functions in
976 head induction. *Nature* **391**, 357-362, doi:10.1038/34848 (1998).

977 37 Pedone, E. & Marucci, L. Role of beta-Catenin Activation Levels and
978 Fluctuations in Controlling Cell Fate. *Genes (Basel)* **10**,
979 doi:10.3390/genes10020176 (2019).

980 38 Aulicino, F., Theka, I., Ombrato, L., Lluis, F. & Cosma, M. P. Temporal
981 perturbation of the Wnt signaling pathway in the control of cell reprogramming
982 is modulated by TCF1. *Stem Cell Reports* **2**, 707-720,
983 doi:10.1016/j.stemcr.2014.04.001 (2014).

984 39 Ho, R., Papp, B., Hoffman, J. A., Merrill, B. J. & Plath, K. Stage-specific
985 regulation of reprogramming to induced pluripotent stem cells by Wnt signaling
986 and T cell factor proteins. *Cell Rep* **3**, 2113-2126,
987 doi:10.1016/j.celrep.2013.05.015 (2013).

988 40 Kimura, M., Nakajima-Koyama, M., Lee, J. & Nishida, E. Transient Expression
989 of WNT2 Promotes Somatic Cell Reprogramming by Inducing beta-Catenin
990 Nuclear Accumulation. *Stem Cell Reports* **6**, 834-843,
991 doi:10.1016/j.stemcr.2016.04.012 (2016).

992 41 Lluis, F., Pedone, E., Pepe, S. & Cosma, M. P. Periodic activation of Wnt/beta-
993 catenin signaling enhances somatic cell reprogramming mediated by cell
994 fusion. *Cell Stem Cell* **3**, 493-507, doi:10.1016/j.stem.2008.08.017 (2008).

995 42 Anton, R., Kestler, H. A. & Kuhl, M. Beta-catenin signaling contributes to
996 stemness and regulates early differentiation in murine embryonic stem cells.
997 *FEBS Lett* **581**, 5247-5254, doi:10.1016/j.febslet.2007.10.012 (2007).

998 43 Soncin, F., Mohamet, L., Eckardt, D., Ritson, S., Eastham, A. M., Bobola, N.,
999 Russell, A., Davies, S., Kemler, R., Merry, C. L. & Ward, C. M. Abrogation of E-
1000 cadherin-mediated cell-cell contact in mouse embryonic stem cells results in

1001 reversible LIF-independent self-renewal. *Stem Cells* **27**, 2069-2080,
1002 doi:10.1002/stem.134 (2009).

1003 44 Wagner, R. T., Xu, X., Yi, F., Merrill, B. J. & Cooney, A. J. Canonical Wnt/beta-
1004 catenin regulation of liver receptor homolog-1 mediates pluripotency gene
1005 expression. *Stem Cells* **28**, 1794-1804, doi:10.1002/stem.502 (2010).

1006 45 Aulicino, F., Sottile, F., Pedone, E., Lluis, F., Marucci, L. & Cosma, M. P.
1007 Canonical Wnt pathway controls mESCs self-renewal through inhibition of
1008 spontaneous differentiation via β -catenin/TCF/LEF functions. *bioRxiv*,
1009 doi:10.1101/661777 (2019).

1010 46 Lyashenko, N., Winter, M., Migliorini, D., Biechele, T., Moon, R. T. & Hartmann,
1011 C. Differential requirement for the dual functions of beta-catenin in embryonic
1012 stem cell self-renewal and germ layer formation. *Nat Cell Biol* **13**, 753-761,
1013 doi:10.1038/ncb2260 (2011).

1014 47 Wray, J., Kalkan, T., Gomez-Lopez, S., Eckardt, D., Cook, A., Kemler, R. &
1015 Smith, A. Inhibition of glycogen synthase kinase-3 alleviates Tcf3 repression of
1016 the pluripotency network and increases embryonic stem cell resistance to
1017 differentiation. *Nat Cell Biol* **13**, 838-845, doi:10.1038/ncb2267 (2011).

1018 48 Kielman, M. F., Rindapaa, M., Gaspar, C., van Poppel, N., Breukel, C., van
1019 Leeuwen, S., Taketo, M. M., Roberts, S., Smits, R. & Fodde, R. Apc modulates
1020 embryonic stem-cell differentiation by controlling the dosage of beta-catenin
1021 signaling. *Nat Genet* **32**, 594-605, doi:10.1038/ng1045 (2002).

1022 49 Pedone, E., Postiglione, L., Aulicino, F., Rocca, D. L., Montes-Olivas, S.,
1023 Khazim, M., di Bernardo, D., Pia Cosma, M. & Marucci, L. A tunable dual-input
1024 system for on-demand dynamic gene expression regulation. *Nat Commun* **10**,
1025 4481, doi:10.1038/s41467-019-12329-9 (2019).

1026 50 Sadot, E., Conacci-Sorrell, M., Zhurinsky, J., Shnizer, D., Lando, Z., Zharhary,
1027 D., Kam, Z., Ben-Ze'ev, A. & Geiger, B. Regulation of S33/S37 phosphorylated
1028 beta-catenin in normal and transformed cells. *J Cell Sci* **115**, 2771-2780 (2002).

1029 51 Kalkan, T., Olova, N., Roode, M., Mulas, C., Lee, H. J., Nett, I., Marks, H.,
1030 Walker, R., Stunnenberg, H. G., Lilley, K. S., Nichols, J., Reik, W., Bertone, P.
1031 & Smith, A. Tracking the embryonic stem cell transition from ground state
1032 pluripotency. *Development* **144**, 1221-1234, doi:10.1242/dev.142711 (2017).

1033 52 Choi, J., Huebner, A. J., Clement, K., Walsh, R. M., Savol, A., Lin, K., Gu, H.,
1034 Di Stefano, B., Brumbaugh, J., Kim, S. Y., Sharif, J., Rose, C. M., Mohammad,

1035 A., Odajima, J., Charron, J., Shioda, T., Gnirke, A., Gygi, S., Koseki, H.,
1036 Sadreyev, R. I., Xiao, A., Meissner, A. & Hochedlinger, K. Prolonged Mek1/2
1037 suppression impairs the developmental potential of embryonic stem cells.
1038 *Nature* **548**, 219-223, doi:10.1038/nature23274 (2017).

1039 53 Parchem, R. J., Ye, J., Judson, R. L., LaRussa, M. F., Krishnakumar, R.,
1040 Blelloch, A., Oldham, M. C. & Blelloch, R. Two miRNA clusters reveal
1041 alternative paths in late-stage reprogramming. *Cell Stem Cell* **14**, 617-631,
1042 doi:10.1016/j.stem.2014.01.021 (2014).

1043 54 Turco, M. Y., Furia, L., Dietze, A., Fernandez Diaz, L., Ronzoni, S., Sciuollo, A.,
1044 Simeone, A., Constam, D., Faretta, M. & Lanfrancone, L. Cellular heterogeneity
1045 during embryonic stem cell differentiation to epiblast stem cells is revealed by
1046 the ShcD/RaLP adaptor protein. *Stem Cells* **30**, 2423-2436,
1047 doi:10.1002/stem.1217 (2012).

1048 55 Zhang, J., Ratanasirinrawoot, S., Chandrasekaran, S., Wu, Z., Ficarro, S. B.,
1049 Yu, C., Ross, C. A., Cacchiarelli, D., Xia, Q., Seligson, M., Shinoda, G., Xie,
1050 W., Cahan, P., Wang, L., Ng, S. C., Tintara, S., Trapnell, C., Onder, T., Loh, Y.
1051 H., Mikkelsen, T., Sliz, P., Teitell, M. A., Asara, J. M., Marto, J. A., Li, H., Collins,
1052 J. J. & Daley, G. Q. LIN28 Regulates Stem Cell Metabolism and Conversion to
1053 Primed Pluripotency. *Cell Stem Cell* **19**, 66-80, doi:10.1016/j.stem.2016.05.009
1054 (2016).

1055 56 Fidalgo, M., Huang, X., Guallar, D., Sanchez-Priego, C., Valdes, V. J.,
1056 Saunders, A., Ding, J., Wu, W. S., Clavel, C. & Wang, J. Zfp281 Coordinates
1057 Opposing Functions of Tet1 and Tet2 in Pluripotent States. *Cell Stem Cell* **19**,
1058 355-369, doi:10.1016/j.stem.2016.05.025 (2016).

1059 57 Luo, Z., Gao, X., Lin, C., Smith, E. R., Marshall, S. A., Swanson, S. K., Florens,
1060 L., Washburn, M. P. & Shilatifard, A. Zic2 is an enhancer-binding factor required
1061 for embryonic stem cell specification. *Mol Cell* **57**, 685-694,
1062 doi:10.1016/j.molcel.2015.01.007 (2015).

1063 58 Betschinger, J., Nichols, J., Dietmann, S., Corrin, P. D., Paddison, P. J. &
1064 Smith, A. Exit from pluripotency is gated by intracellular redistribution of the
1065 bHLH transcription factor Tfe3. *Cell* **153**, 335-347,
1066 doi:10.1016/j.cell.2013.03.012 (2013).

1067 59 Brandenberger, R., Wei, H., Zhang, S., Lei, S., Murage, J., Fisk, G. J., Li, Y.,
1068 Xu, C., Fang, R., Guegler, K., Rao, M. S., Mandalam, R., Lebkowski, J. &

1069 Stanton, L. W. Transcriptome characterization elucidates signaling networks
1070 that control human ES cell growth and differentiation. *Nat Biotechnol* **22**, 707-
1071 716, doi:10.1038/nbt971 (2004).

1072 60 Wang, Z. X., Teh, C. H., Chan, C. M., Chu, C., Rossbach, M., Kunarso, G.,
1073 Allapitchay, T. B., Wong, K. Y. & Stanton, L. W. The transcription factor Zfp281
1074 controls embryonic stem cell pluripotency by direct activation and repression of
1075 target genes. *Stem Cells* **26**, 2791-2799, doi:10.1634/stemcells.2008-0443
1076 (2008).

1077 61 Mayer, D., Stadler, M. B., Rittirsch, M., Hess, D., Lukonin, I., Winzi, M., Smith,
1078 A., Buchholz, F. & Betschinger, J. Zfp281 orchestrates interconversion of
1079 pluripotent states by engaging Ehmt1 and Zic2. *EMBO J* **39**, e102591,
1080 doi:10.15252/embj.2019102591 (2020).

1081 62 Okuda, A., Fukushima, A., Nishimoto, M., Orimo, A., Yamagishi, T.,
1082 Nabeshima, Y., Kuro-o, M., Nabeshima, Y., Boon, K., Keaveney, M.,
1083 Stunnenberg, H. G. & Muramatsu, M. UTF1, a novel transcriptional coactivator
1084 expressed in pluripotent embryonic stem cells and extra-embryonic cells.
EMBO J **17**, 2019-2032, doi:10.1093/emboj/17.7.2019 (1998).

1086 63 Kooistra, S. M., Thummer, R. P. & Eggen, B. J. Characterization of human
1087 UTF1, a chromatin-associated protein with repressor activity expressed in
1088 pluripotent cells. *Stem Cell Res* **2**, 211-218, doi:10.1016/j.scr.2009.02.001
1089 (2009).

1090 64 Jia, J., Zheng, X., Hu, G., Cui, K., Zhang, J., Zhang, A., Jiang, H., Lu, B., Yates,
1091 J., 3rd, Liu, C., Zhao, K. & Zheng, Y. Regulation of pluripotency and self-
1092 renewal of ESCs through epigenetic-threshold modulation and mRNA pruning.
Cell **151**, 576-589, doi:10.1016/j.cell.2012.09.023 (2012).

1094 65 Respuela, P., Nikolic, M., Tan, M., Frommolt, P., Zhao, Y., Wysocka, J. & Rada-
1095 Iglesias, A. Foxd3 Promotes Exit from Naive Pluripotency through Enhancer
1096 Decommissioning and Inhibits Germline Specification. *Cell Stem Cell* **18**, 118-
1097 133, doi:10.1016/j.stem.2015.09.010 (2016).

1098 66 Yasunaga, M., Tada, S., Torikai-Nishikawa, S., Nakano, Y., Okada, M., Jakt, L.
1099 M., Nishikawa, S., Chiba, T., Era, T. & Nishikawa, S. Induction and monitoring
1100 of definitive and visceral endoderm differentiation of mouse ES cells. *Nat
1101 Biotechnol* **23**, 1542-1550, doi:10.1038/nbt1167 (2005).

1102 67 Engert, S., Burtscher, I., Liao, W. P., Dulev, S., Schotta, G. & Lickert, H.
1103 Wnt/beta-catenin signalling regulates Sox17 expression and is essential for
1104 organizer and endoderm formation in the mouse. *Development* **140**, 3128-
1105 3138, doi:10.1242/dev.088765 (2013).

1106 68 Tasic, J., Kim, G. J., Pavlovic, M., Schroder, C. M., Mersiowsky, S. L., Barg,
1107 M., Hofherr, A., Probst, S., Kottgen, M., Hein, L. & Arnold, S. J. Eomes and
1108 Brachyury control pluripotency exit and germ-layer segregation by changing the
1109 chromatin state. *Nat Cell Biol* **21**, 1518-1531, doi:10.1038/s41556-019-0423-1
1110 (2019).

1111 69 Ying, Q. L., Stavridis, M., Griffiths, D., Li, M. & Smith, A. Conversion of
1112 embryonic stem cells into neuroectodermal precursors in adherent
1113 monoculture. *Nat Biotechnol* **21**, 183-186, doi:10.1038/nbt780 (2003).

1114 70 Langfelder, P. & Horvath, S. WGCNA: an R package for weighted correlation
1115 network analysis. *BMC Bioinformatics* **9**, 559, doi:10.1186/1471-2105-9-559
1116 (2008).

1117 71 Ogawa, K., Nishinakamura, R., Iwamatsu, Y., Shimosato, D. & Niwa, H.
1118 Synergistic action of Wnt and LIF in maintaining pluripotency of mouse ES cells.
1119 *Biochem Biophys Res Commun* **343**, 159-166, doi:10.1016/j.bbrc.2006.02.127
1120 (2006).

1121 72 Hao, J., Li, T. G., Qi, X., Zhao, D. F. & Zhao, G. Q. WNT/beta-catenin pathway
1122 up-regulates Stat3 and converges on LIF to prevent differentiation of mouse
1123 embryonic stem cells. *Dev Biol* **290**, 81-91, doi:10.1016/j.ydbio.2005.11.011
1124 (2006).

1125 73 Singla, D. K., Schneider, D. J., LeWinter, M. M. & Sobel, B. E. wnt3a but not
1126 wnt11 supports self-renewal of embryonic stem cells. *Biochem Biophys Res
1127 Commun* **345**, 789-795, doi:10.1016/j.bbrc.2006.04.125 (2006).

1128 74 Takao, Y., Yokota, T. & Koide, H. Beta-catenin up-regulates Nanog expression
1129 through interaction with Oct-3/4 in embryonic stem cells. *Biochem Biophys Res
1130 Commun* **353**, 699-705, doi:10.1016/j.bbrc.2006.12.072 (2007).

1131 75 Tsukiyama, T. & Ohinata, Y. A modified EpiSC culture condition containing a
1132 GSK3 inhibitor can support germline-competent pluripotency in mice. *PLoS
1133 One* **9**, e95329, doi:10.1371/journal.pone.0095329 (2014).

1134 76 Sugimoto, M., Kondo, M., Koga, Y., Shiura, H., Ikeda, R., Hirose, M., Ogura,
1135 A., Murakami, A., Yoshiki, A., Chuva de Sousa Lopes, S. M. & Abe, K. A simple

1136 and robust method for establishing homogeneous mouse epiblast stem cell
1137 lines by wnt inhibition. *Stem Cell Reports* **4**, 744-757,
1138 doi:10.1016/j.stemcr.2015.02.014 (2015).

1139 77 Sumi, T., Oki, S., Kitajima, K. & Meno, C. Epiblast ground state is controlled by
1140 canonical Wnt/beta-catenin signaling in the postimplantation mouse embryo
1141 and epiblast stem cells. *PLoS One* **8**, e63378,
1142 doi:10.1371/journal.pone.0063378 (2013).

1143 78 Liu, K., Sun, Y., Liu, D. & Ye, S. Inhibition of Wnt/beta-catenin signaling by
1144 IWR1 induces expression of Foxd3 to promote mouse epiblast stem cell self-
1145 renewal. *Biochem Biophys Res Commun* **490**, 616-622,
1146 doi:10.1016/j.bbrc.2017.06.086 (2017).

1147 79 Osteil, P., Studdert, J. B., Goh, H. N., Wilkie, E. E., Fan, X., Khoo, P. L., Peng,
1148 Salehin, N., Knowles, H., Han, J. J., Jing, N., Fossat, N. & Tam, P. P. L.
1149 Dynamics of Wnt activity on the acquisition of ectoderm potency in epiblast
1150 stem cells. *Development* **146**, doi:10.1242/dev.172858 (2019).

1151 80 Kurek, D., Neagu, A., Tastemel, M., Tuysuz, N., Lehmann, J., van de Werken,
1152 H. J. G., Philipsen, S., van der Linden, R., Maas, A., van, I. W. F. J., Drukker,
1153 M. & Ten Berge, D. Endogenous WNT signals mediate BMP-induced and
1154 spontaneous differentiation of epiblast stem cells and human embryonic stem
1155 cells. *Stem Cell Reports* **4**, 114-128, doi:10.1016/j.stemcr.2014.11.007 (2015).

1156 81 Munoz Descalzo, S., Rue, P., Garcia-Ojalvo, J. & Martinez Arias, A.
1157 Correlations between the levels of Oct4 and Nanog as a signature for naive
1158 pluripotency in mouse embryonic stem cells. *Stem Cells* **30**, 2683-2691,
1159 doi:10.1002/stem.1230 (2012).

1160 82 Dobin, A., Davis, C. A., Schlesinger, F., Drenkow, J., Zaleski, C., Jha, S., Batut,
1161 P., Chaisson, M. & Gingeras, T. R. STAR: ultrafast universal RNA-seq aligner.
1162 *Bioinformatics* **29**, 15-21, doi:10.1093/bioinformatics/bts635 (2013).

1163 83 Anders, S., Pyl, P. T. & Huber, W. HTSeq--a Python framework to work with
1164 high-throughput sequencing data. *Bioinformatics* **31**, 166-169,
1165 doi:10.1093/bioinformatics/btu638 (2015).

1166 84 Robinson, M. D., McCarthy, D. J. & Smyth, G. K. edgeR: a Bioconductor
1167 package for differential expression analysis of digital gene expression data.
1168 *Bioinformatics* **26**, 139-140, doi:10.1093/bioinformatics/btp616 (2010).

1169 85 Yip, A. M. & Horvath, S. Gene network interconnectedness and the generalized
1170 topological overlap measure. *BMC Bioinformatics* **8**, 22, doi:10.1186/1471-
1171 2105-8-22 (2007).

1172 86 Langfelder, P., Zhang, B. & Horvath, S. Defining clusters from a hierarchical
1173 cluster tree: the Dynamic Tree Cut package for R. *Bioinformatics* **24**, 719-720,
1174 doi:10.1093/bioinformatics/btm563 (2008).

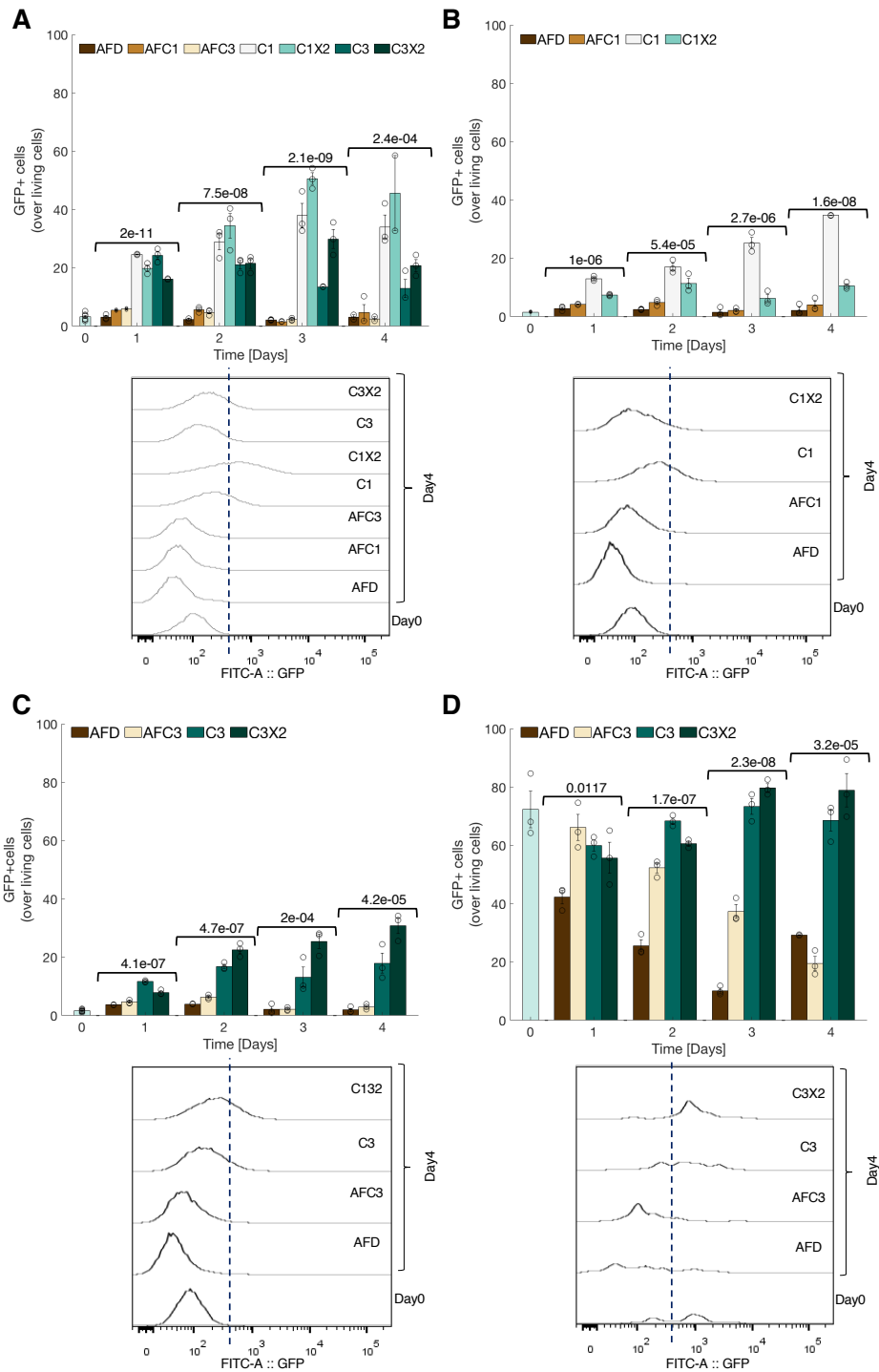
1175 87 Hubert, L., Arabie, P. . Comparing partitions. *Journal of Classification* **2**, 193-
1176 218, doi:10.1007/BF01908075 (1985).

1177 88 Ashburner, M., Ball, C. A., Blake, J. A., Botstein, D., Butler, H., Cherry, J. M.,
1178 Davis, A. P., Dolinski, K., Dwight, S. S., Eppig, J. T., Harris, M. A., Hill, D. P.,
1179 Issel-Tarver, L., Kasarskis, A., Lewis, S., Matese, J. C., Richardson, J. E.,
1180 Ringwald, M., Rubin, G. M. & Sherlock, G. Gene ontology: tool for the
1181 unification of biology. The Gene Ontology Consortium. *Nat Genet* **25**, 25-29,
1182 doi:10.1038/75556 (2000).

1183 89 Kanehisa, M. & Goto, S. KEGG: kyoto encyclopedia of genes and genomes.
1184 *Nucleic Acids Res* **28**, 27-30, doi:10.1093/nar/28.1.27 (2000).

1185 90 Yu, G., Wang, L. G., Han, Y. & He, Q. Y. clusterProfiler: an R package for
1186 comparing biological themes among gene clusters. *OMICS* **16**, 284-287,
1187 doi:10.1089/omi.2011.0118 (2012).

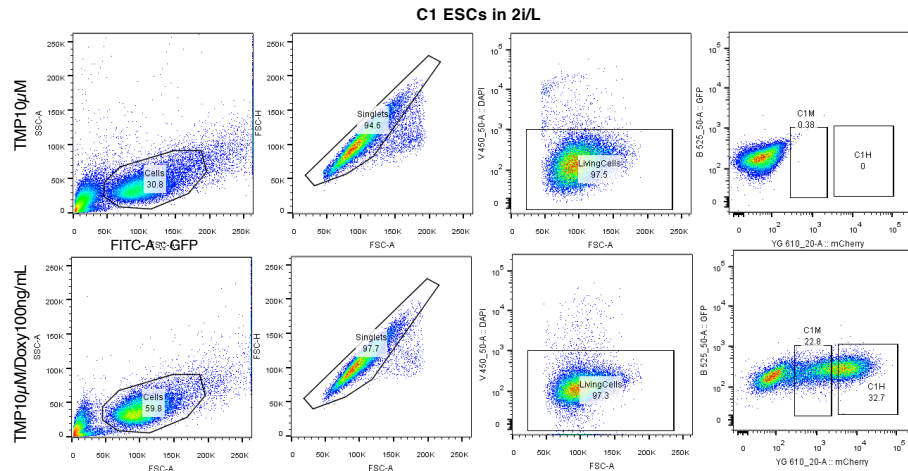
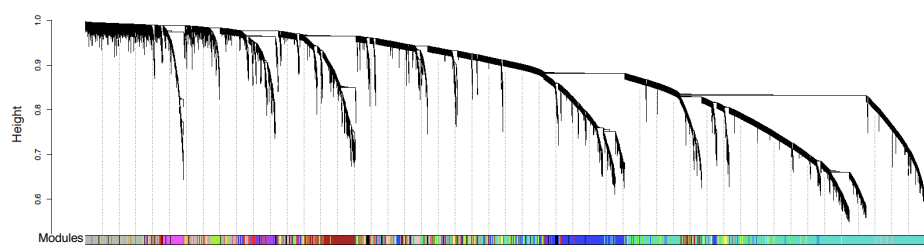
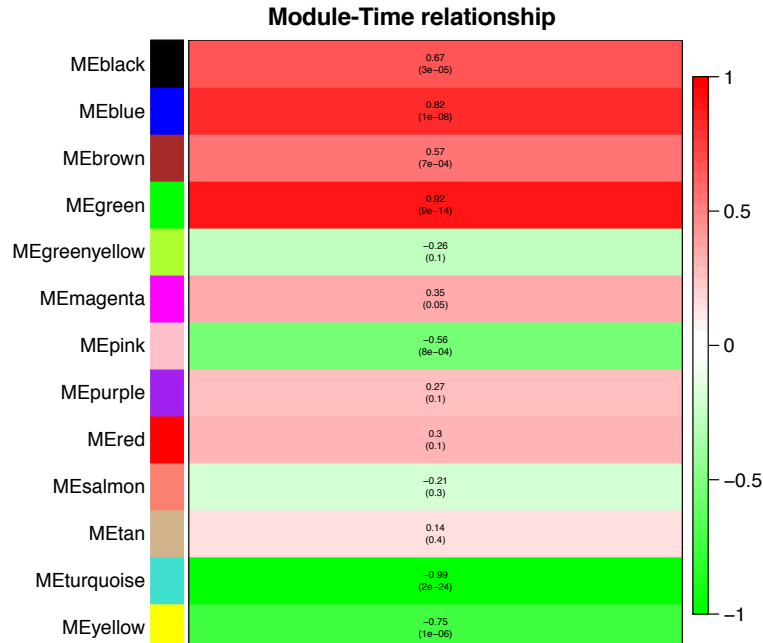
1188



1189 **Supplementary Figure 2. Replica of *in vitro* ESC-EpiSC differentiation**
1190 **experiments upon chemical β-catenin perturbations**

1191 **A-D** Percentage of GFP+ cells calculated over the total amount of leaving cells in
1192 DMSO (**B**), Ch1μM (**C**), Ch3μM (**D**) and 2i/L (**E**) pre-cultured dual reporter ESCs.
1193 Histograms from Day 0 and Day 4 of each condition are shown as inset. Data are
1194 means±SEM (n=2, A (Day1 C1, Day3 AFC1, Day4 AFD-AFC3), B (Day 1 AFC1), D
1195 (Day4 AFD); n=3, A (Day1 AFD-AFC1-AFC3-C1X2-C3-C3X2, Day2, Day3 AFD-

1196 AFC3-C1-C1X2-C3-C3X2, Day4 AFC1-C1-C1X2-C3-C3X2), B (Day1 AFD-C1-C1X2,
1197 Day2, Day3, Day4), C (Day1, Day2, Day3, Day4), D (Day0, Day1, Day2, Day3, Day4);
1198 n=6, A (Day0), B (Day0), C (Day0). p-values from one-way ANOVA are shown across
1199 samples for each day. Dots represent individual data with similar values overlapping.
1200 Colour-blind safe combinations were selected using colorbrewer2
1201 (<https://colorbrewer2.org/#type=sequential&scheme=BuGn&n=3>).
1202
1203
1204
1205
1206
1207
1208
1209
1210
1211
1212
1213
1214
1215
1216

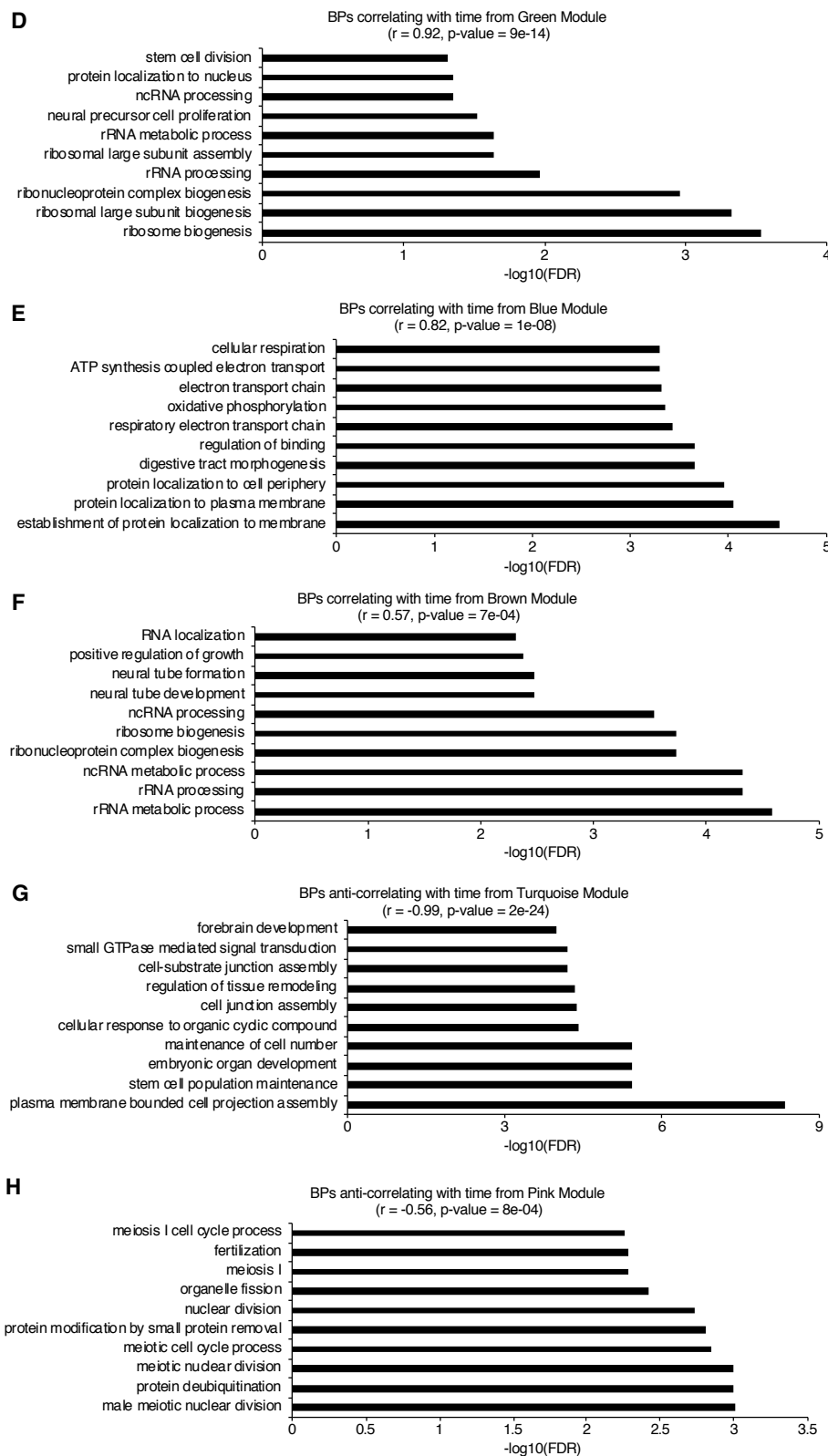
A**B****C**

1217

1218

1219

1220



1221 **Supplementary Figure 3. FACS gating strategy and WGCNA of the genes**
 1222 **correlating with time.**

1223 **A** Gating strategy used to sort C1M and C1H ESCs, following 48 hrs treatment with
 1224 TMP10 μ M and Doxy100ng/mL. C1 ESCs treated with TMP10 μ M were used as
 1225 negative control. **B** Clustering dendrogram of genes, with dissimilarity based on

1226 topological overlap, together with the assigned module colours; grey genes are
1227 unassigned to any module. **C** Eigenmodules correlating with time; the Pearson
1228 correlation coefficient (r) and relative p-value are shown. **D-H** Bar-chart of the top-ten
1229 enriched biological processes (BP) with FDR < 0.05 from genes belonging to the
1230 Green (**D**), Blue (**E**), Brown (**F**), turquoise (**G**) and Pink (**H**) WGCNA modules.

1231

1232

1233

1234

1235

1236

1237

1238

1239

1240

1241

1242

1243

1244

1245

1246

1247

1248

1249

1250

1251

1252

1253

1254

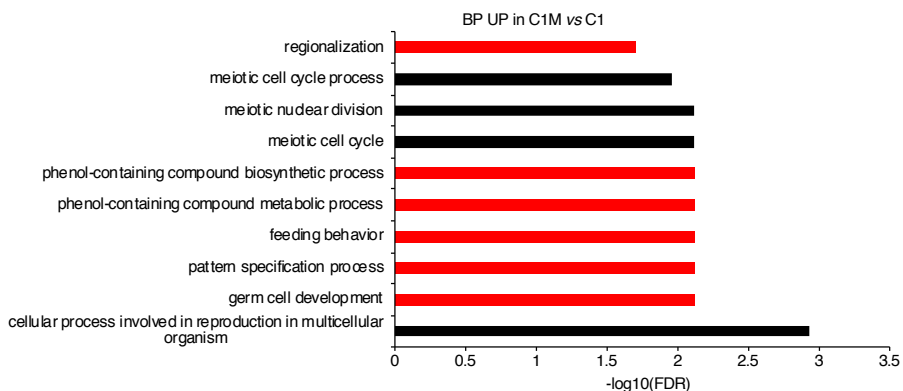
1255

1256

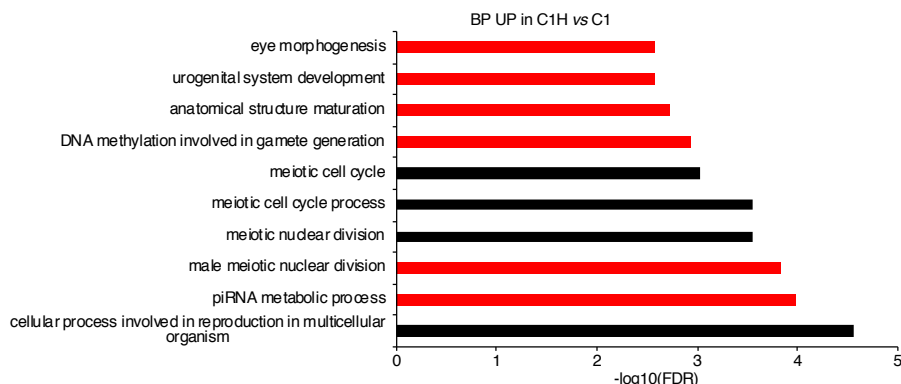
1257

1258

A



B



1259 **Supplementary Figure 4. Gene ontology of the differential expressed genes in**
1260 **pluripotent ESCs.**

1261 **A, B** Bar-chart of the top-ten enriched biological processes (BP) with FDR < 0.05 from
1262 differentially expressed genes in in C1M (**A**) and C1H (**B**) compared to C1 ESCs. Black
1263 and grey bars represent upregulated and downregulated BPs, respectively. In red
1264 bars, the BPs exclusively enriched in the indicated condition.

1265

1266 **Supplementary Table 1**

1267 List of identified module genes correlating with time (Supplementary Figure 3) or β -
1268 catenin doses (Figure 3) before and after the filtering for the $|kME| \geq 0.8$; GO and
1269 pathway analysis.

1270

1271 **Supplementary Table 2**

1272 List of differentially expressed genes before and after the filtering for the FDR (< 0.05)
1273 and log fold change (-2 > log > 2); GO and pathway analysis in pluripotent C1M vs C1
1274 ESCs.

1275

1276 **Supplementary Table 3**

1277 List of differentially expressed genes before and after the filtering for the FDR (< 0.05)
1278 and log fold change (-2 > log > 2); GO and pathway analysis in pluripotent C1H vs C1
1279 ESCs.

1280

1281 **Supplementary Table 4**

1282 List of differentially expressed genes before and after the filtering for the FDR (< 0.05)
1283 and log fold change (-2 > log > 2); GO and pathway analysis in differentiated C1DMV
1284 vs C1D ESCs.

1285

1286 **Supplementary Table 5**

1287 List of differentially expressed genes before and after the filtering for the FDR (< 0.05)
1288 and log fold change (-2 > log > 2); GO and pathway analysis in differentiated C1DMDT
1289 vs C1D ESCs.

1290

1291 **Supplementary Table 6**

1292 List of differentially expressed genes before and after the filtering for the FDR (< 0.05)
1293 and log fold change (-2 > log > 2); GO and pathway analysis in differentiated C1HV vs
1294 C1D ESCs.

1295

1296 **Supplementary Table 7**

1297 List of differentially expressed genes before and after the filtering for the FDR (< 0.05)
1298 and log fold change (-2 > log > 2); GO and pathway analysis in differentiated C1DHDT
1299 vs C1D ESCs.

1300

1301 **Supplementary Movie 1**

1302 71 hrs time-lapse of dual reporter ESCs without pre-activation of the canonical Wnt
1303 pathway, differentiated in NDiff227 supplemented with ActivinA+Fgf2+DMSO.

1304

1305 **Supplementary Movie 2**

1306 71 hrs time-lapse of dual reporter ESCs without pre-activation of the canonical Wnt
1307 pathway, differentiated in NDiff227 supplemented with Chiron 1 μ M.

1308

1309 **Supplementary Movie 3**

1310 71 hrs time-lapse of dual reporter ESCs without pre-activation of the canonical Wnt
1311 pathway, differentiated in NDiff227 supplemented with Chiron 3 μ M.
1312